

---

# NON-NEGATIVE BREGMAN DIVERGENCE MINIMIZATION FOR DEEP DIRECT DENSITY RATIO ESTIMATION

---

A PREPRINT

**Masahiro Kato**  
CyberAgent Inc.  
Tokyo, Japan  
masahiro\_kato@cyberagent.co.jp

**Takeshi Teshima**  
The University of Tokyo  
Tokyo, Japan  
teshima@ms.k.u-tokyo.ac.jp

June 15, 2020

## ABSTRACT

The estimation of the ratio of two probability densities has garnered attention as the *density ratio* is useful in various machine learning tasks, such as anomaly detection and domain adaptation. To estimate the density ratio, methods collectively known as *direct density ratio estimation* (DRE) have been explored. These methods are based on the minimization of the *Bregman* (BR) divergence between a density ratio model and the true density ratio. However, existing direct DRE suffers from serious *overfitting* when using *flexible models* such as neural networks. In this paper, we introduce a *non-negative correction* for empirical risk using only the prior knowledge of the *upper bound of the density ratio*. This correction makes a DRE method more robust against overfitting and enables the use of flexible models. In the theoretical analysis, we discuss the consistency of the empirical risk. In our experiments, the proposed estimators show favorable performance in inlier-based outlier detection and covariate shift adaptation.

## 1 Introduction

The ratio of probability densities has been used in various industrial applications (Sugiyama et al., 2009, 2012), such as anomaly detection (Hido et al., 2011; Smola et al., 2009; Abe & Sugiyama, 2019), two-sample testing (Keziou & Leoni-Aubin, 2005; Sugiyama et al., 2011a), off-policy evaluation (Kato et al., 2020), change detection in time series (Kawahara & Sugiyama, 2009), and binary classification only from positive and unlabeled data (PU learning; Kato et al., 2019). Thus, the estimation of the density ratio has attracted a great deal of attention. A naive approach is to estimate the two densities of the numerator and denominator separately, then take the ratio of the estimated densities. However, this approach is difficult to apply to high-dimensional data as division by an estimated quantity can magnify the estimation error in the numerator. To overcome this drawback, various approaches of direct DRE have been explored without undergoing density estimation. These approaches include the moment matching (Huang et al., 2007; Gretton et al., 2009), the probabilistic classification (Qin, 1998; Cheng & Chu, 2004), the density matching (Nguyen et al., 2011; Yamada et al., 2010), and the density-ratio fitting (Kanamori et al., 2009). Sugiyama et al. (2011b) showed that these methods could be generalized as density ratio matching under the Bregman (BR) divergence (Bregman, 1967). Recently, Kato et al. (2019) also proposed using the risk for PU learning proposed by du Plessis et al. (2015) for DRE, which also can be generalized from the viewpoint of BR divergence minimization as we show below.

However, a serious *overfitting* problem is often observed when we minimize an empirically approximated BR divergence with respect to a flexible density ratio model such as neural networks. This is caused because there is no lower bound in the empirically approximated BR divergence, i.e., we can achieve an infinitely negative value in minimization. In existing DRE methods, this problem has been rarely discussed. One reason for this is that the existing method often assumes a linear-in-parameter model to approximate the density ratio (Kanamori et al., 2012), which is not so flexible compared with neural networks. On the other hand, recent developments in machine learning suggest that using neural networks has significantly improved the performances for various tasks, such as computer vision

Table 1: Summary of methods for DRE(Sugiyama et al., 2011b). For PULogLoss, we use  $C < \frac{1}{R}$ .

Method	$f(t)$	Reference
LSIF	$(t-1)^2/2$	Kanamori et al. (2009)
KLIEP (UKL)	$t \log(t) - t$	Sugiyama et al. (2008)
Kernel Mean Matching	$(t-1)^2/2$	Gretton et al. (2009)
Logistic Regression (BKL)	$t \log(t) - (1+t) \log(1+t)$	Hastie et al. (2001)
PULogLoss	$\log(1-t) + Ct(\log(t) - \log(1-t))$ for $0 < t < 1$	Kato et al. (2019)

(Krizhevsky et al., 2012) and natural language processing (Bengio et al., 2001). Thus, we have the motivation to use neural networks to approximate the density ratio.

To mitigate the overfitting, we propose a general procedure to modify the empirical BR divergence using only the prior knowledge of the upper bound of the density ratio. Our idea of the correction has been inspired by Kiryo et al. (2017), which proposed using non-negative correction to the empirical risk of classification for using neural networks in PU learning. However, the idea of non-negative correction is only immediately applicable to the binary classification risk, thus we require a non-trivial rewriting of the BR divergence to generalize the approach to our problem. In analogy to Kiryo et al. (2017), we call the proposed empirical risk the *non-negative BR* (nnBR) divergence, and it can be regarded as a generalization of the risk for PU learning with flexible models proposed by Kiryo et al. (2017).

Our main contributions are: (1) the proposal of a general procedure to modify a BR divergence to enable DRE with flexible models, (2) theoretical justification of the proposed estimator, and (3) the experimental validation of the proposed method using benchmark data.

## 2 Problem Setting

Let  $\mathcal{X}^{\text{nu}} \subseteq \mathbb{R}^d$  and  $\mathcal{X}^{\text{de}} \subseteq \mathbb{R}^d$  be the domains of the  $d$ -dimensional *covariates*  $\{\mathbf{x}_i^{\text{nu}}\}_{i=1}^{n_{\text{nu}}}$  and  $\{\mathbf{x}_i^{\text{de}}\}_{i=1}^{n_{\text{de}}}$ , respectively, which are independent and identically distributed (i.i.d.) as  $\{\mathbf{x}_i^{\text{nu}}\}_{i=1}^{n_{\text{nu}}} \stackrel{\text{i.i.d.}}{\sim} p_{\text{nu}}(\mathbf{x})$  and  $\{\mathbf{x}_i^{\text{de}}\}_{i=1}^{n_{\text{de}}} \stackrel{\text{i.i.d.}}{\sim} p_{\text{de}}(\mathbf{x})$ , where  $p_{\text{nu}}(\mathbf{x})$  and  $p_{\text{de}}(\mathbf{x})$  are probability densities over  $\mathcal{X}^{\text{nu}}$  and  $\mathcal{X}^{\text{de}}$ , respectively. Here, “nu” and “de” indicate the numerator and the denominator. Our goal is to estimate the density ratio  $r^*(\mathbf{x}) = \frac{p_{\text{nu}}(\mathbf{x})}{p_{\text{de}}(\mathbf{x})}$ . To identify the density ratio, we assume the following:

**Assumption 1.** The density  $p_{\text{nu}}(\mathbf{x})$  is strictly positive over the domain  $\mathcal{X}^{\text{nu}}$ , the density  $p_{\text{de}}(\mathbf{x})$  is strictly positive over the domain  $\mathcal{X}^{\text{de}}$ , and  $\mathcal{X}^{\text{nu}} \subseteq \mathcal{X}^{\text{de}}$ . In addition, the density ratio  $r^*(\mathbf{x})$  is bounded from above:  $\overline{R} = \sup_{\mathbf{x}} r^*(\mathbf{x}) < \infty$ .

**Notation:** Let  $\mathbb{E}_{\text{nu}}$  and  $\mathbb{E}_{\text{de}}$  denote the expectations over  $p_{\text{nu}}(\mathbf{x})$  and  $p_{\text{de}}(\mathbf{x})$ , respectively. Let  $\hat{\mathbb{E}}_{\text{nu}}$  and  $\hat{\mathbb{E}}_{\text{de}}$  denote the sample average over  $\{\mathbf{x}_i^{\text{nu}}\}_{i=1}^{n_{\text{nu}}}$  and  $\{\mathbf{x}_i^{\text{de}}\}_{i=1}^{n_{\text{de}}}$ , respectively. Let  $\mathcal{H} \subset \{r : \mathbb{R}^d \rightarrow (b_r, B_r)\}$  be the hypothesis class of the density ratio, where  $0 \leq b_r < \overline{R} < B_r$ .

### 2.1 Density Ratio Matching under the Bregman Divergence

A naive way to implement DRE would be to estimate the numerator and the denominator densities separately and take the ratio. However, according to Vapnik’s principle, we should avoid solving a more difficult intermediate problem than the target problem (Vapnik, 1998). Therefore, various methods for directly estimating the density ratio model have been proposed (Sugiyama et al., 2012), and Sugiyama et al. (2011b) showed that those methods can be generalized from the viewpoint of the *density ratio matching under the BR divergence*.

The BR divergence is an extension of the Euclidean distance to a class of divergences that share similar properties (Bregman, 1967). Formally, let  $f : (b_r, B_r) \rightarrow \mathbb{R}$  be a twice continuously differentiable convex function with a bounded derivative. Then, the point-wise BR divergence associated with  $f$  from  $t^*$  to  $t$  is defined as  $\text{BR}'_f(t^*||t) := f(t^*) - f(t) - \partial f(t)(t^* - t)$ , where  $\partial f$  is the derivative of  $f$ . Now, the discrepancy from the true density ratio function  $r^*$  to a density ratio model  $r$  is measured by integrating the point-wise BR divergence as follows (Sugiyama et al., 2011b):

$$\text{BR}'_f(r^*||r) := \int p_{\text{de}}(\mathbf{x}) (f(r^*(\mathbf{x})) - f(r(\mathbf{x})) - \partial f(r(\mathbf{x}))(r^*(\mathbf{x}) - r(\mathbf{x}))) d\mathbf{x}. \quad (1)$$

We estimate the density ratio by finding a function  $f$  that minimizes the BR divergence defined in (1). Here, we subtract the constant  $\overline{\text{BR}} = \mathbb{E}_{\text{de}}[f(r^*(\mathbf{x}))]$  from (1) to obtain

$$\text{BR}_f(r^*||r) := \int p_{\text{de}}(\mathbf{x}) \left( \partial f(r(\mathbf{x}))r(\mathbf{x}) - f(r(\mathbf{x})) \right) d\mathbf{x} - \int p_{\text{nu}}(\mathbf{x}) \partial f(r(\mathbf{x})) d\mathbf{x}. \quad (2)$$

Since  $\overline{\text{BR}}$  is constant with respect to  $r$ , we have  $\arg \min_r \text{BR}'_f(r^*||r) = \arg \min_r \text{BR}_f(r^*||r)$ . Then, let us define the sample analogue of (2) as

$$\widehat{\text{BR}}_f(r) := \hat{\mathbb{E}}_{\text{nu}} \left[ \partial f(r(\mathbf{x}_i))r(\mathbf{x}_i) - f(r(\mathbf{x}_i)) \right] - \hat{\mathbb{E}}_{\text{de}} \left[ \partial f(r(\mathbf{x}_j)) \right]. \quad (3)$$

For a hypothesis class  $\mathcal{H}$ , we estimate the density ratio by solving  $\min_{r \in \mathcal{H}} \widehat{\text{BR}}_f(r^*||r)$ .

**Examples of DRE:** Sugiyama et al. (2011b) showed that various DRE methods can be unified from the viewpoint of BR divergence minimization. Furthermore, Menon & Ong (2016) showed an equivalence between conditional probability estimation and DRE by BR divergence minimization. In addition, we can derive a novel method for DRE from the proposed method of du Plessis et al. (2015) and Kato et al. (2019). We summarize the DRE methods in Table 1. Here, we introduce the empirical risks of *least-square importance fitting* (LSIF), the *Kullback–Leibler importance estimation procedure* (KLIEP), logistic regression (LR), and *PU learning with log Loss* (PULogLoss):

$$\begin{aligned} \widehat{\text{BR}}_{\text{LSIF}}(r) &:= \hat{\mathbb{E}}_{\text{nu}}[r(X)] + \frac{1}{2} \hat{\mathbb{E}}_{\text{de}}[(r(X))^2], \quad \widehat{\text{BR}}_{\text{UKL}}(r) := \hat{\mathbb{E}}_{\text{de}}[r(X)] - \hat{\mathbb{E}}_{\text{nu}}[\log(r(\mathbf{x}))], \\ \widehat{\text{BR}}_{\text{BKL}}(r) &:= -\hat{\mathbb{E}}_{\text{de}} \left[ \log \left( \frac{1}{1+r(X)} \right) \right] - \hat{\mathbb{E}}_{\text{nu}} \left[ \log \left( \frac{r(X)}{1+r(\mathbf{x})} \right) \right], \\ \widehat{\text{BR}}_{\text{PU}}(r) &:= -\hat{\mathbb{E}}_{\text{de}}[\log(1-r(\mathbf{x}_i))] + C \hat{\mathbb{E}}_{\text{nu}}[-\log(r(\mathbf{x}_i)) + \log(1-r(\mathbf{x}_j))], \end{aligned}$$

where  $0 < C < \frac{1}{R}$ . Here,  $\widehat{\text{BR}}_{\text{LSIF}}(r)$  and  $\widehat{\text{BR}}_{\text{PU}}(r)$  correspond to LSIF and PULogLoss, respectively. We can derive the KLIEP and LR from  $\widehat{\text{BR}}_{\text{UKL}}(r)$  and  $\widehat{\text{BR}}_{\text{BKL}}(r)$ , which are called unnormalized Kullback–Leibler (UKL) divergence and binary Kullback–Leibler (BKL) divergence, respectively (Sugiyama et al., 2011b). In  $\widehat{\text{BR}}_{\text{PU}}(r)$ , we restrict the model as  $r \in (0, 1)$  and we obtain an estimator of  $Cr^*$  as a result of the minimization of the risk. Details of the existing methods are shown in Appendix A.

### 3 Deep Direct DRE based on Non-negative Risk Estimator

In this section, we develop methods for DRE with flexible models such as neural networks.

#### 3.1 Difficulties of DRE using Neural Networks

Nam & Sugiyama (2015) and Abe & Sugiyama (2019) approximated the density ratio with neural networks, and Uehara et al. (2016) applied direct DRE for generative adversarial nets (GANs; Goodfellow et al., 2014). In these studies, they trained models based on neural networks by minimizing the empirical BR divergence (3). However, as shown in Section 5, LSIF with neural networks (Nam & Sugiyama, 2015) is numerically unstable due to overfitting. Furthermore, we observed that the overfitting was caused by the following two problems. The first problem is that the empirical BR divergence (3) is not lower bounded: if we use a highly flexible complex hypothesis class  $\mathcal{H}$  and a convex function  $f$ , the term  $-\hat{\mathbb{E}}_{\text{de}}[\partial f(r(\mathbf{x}_j))]$  which is not lower bounded may easily diverge to  $-\infty$  when we minimize (3).

#### 3.2 Non-negative BR Divergence

Although DRE using flexible models suffers from serious overfitting, we still have a strong motivation to use those models for analyzing data such as computer vision and text data. To alleviate the overfitting problem, we propose the *non-negative BR divergence estimator*. The proposed method is inspired by Kiryo et al. (2017), which suggested a non-negative correction to the empirical risk of PU learning based on the knowledge that a part of the population risk is non-negative. On the other hand, in DRE, it is not obvious how to correct the empirical risk because we do not know which part of the population risk (2) is non-negative. However, this can be alleviated by determining the upper bound  $\overline{R}$  of the density ratio  $r^*$ . With the prior knowledge of  $\overline{R}$ , we can determine part of the risk of DRE (2) is non-negative

and conduct a non-negative correction to the empirical risk (3) based on the non-negativity of the population risk. Let us define  $\tilde{f}$  to be a function such that

$$\partial f(t) = C(\partial f(t)t - f(t)) + \tilde{f}(t), \quad (4)$$

where  $0 < C < \frac{1}{\bar{R}}$  and put the following assumption.

**Assumption 2.** We assume that  $\tilde{f}(t)$  is bounded from above and that  $\partial f(t)t - f(t)$  is non-negative.

Assumption 2 is satisfied by most of the loss functions which appear in the previously proposed DRE methods (see Appendix B for examples). Under Assumption 2, because  $\tilde{f}(t)$  is bounded above, the overfitting  $-\hat{\mathbb{E}}_{\text{de}}[\partial f(r(\mathbf{x}_j))] \rightarrow -\infty$  in the minimization of the empirical risk (3) is caused by  $-\hat{\mathbb{E}}_{\text{de}}[C\{\partial f(r(\mathbf{x}_j)) - f(r(\mathbf{x}_j))\}] \rightarrow -\infty$ . Thus, we succeeded in identifying the part of the empirical risk causing the overfitting. Next, to avoid the overfitting, we impose a non-negative correction to the empirical risk (3). First, we rewrite the population risk (2) as

$$\text{BR}_f(r^* \| r) = \int \left\{ p_{\text{de}}(\mathbf{x}) - Cp_{\text{nu}}(\mathbf{x}) \right\} \left\{ \partial f(r(\mathbf{x}))r(\mathbf{x}) - f(r(\mathbf{x})) \right\} d\mathbf{x} - \int p_{\text{nu}}(\mathbf{x}) \left\{ \tilde{f}(r(\mathbf{x})) \right\} d\mathbf{x}.$$

Here, let us  $\ell_1(t) := \partial f(t)t - f(t)$ , and  $\ell_2(t) := -\tilde{f}(t)$ . In the above equation, since Assumption 2 implies  $\ell_1(t) \geq 0$  and  $0 < C < \frac{1}{\bar{R}}$  implies  $\frac{p_{\text{nu}}(\mathbf{x})}{p_{\text{de}}(\mathbf{x})} \leq \bar{R}$  for all  $\mathbf{x} \in \mathcal{X}$ , we have

$$\int \left\{ p_{\text{de}}(\mathbf{x}) - Cp_{\text{nu}}(\mathbf{x}) \right\} \left\{ \ell_1(r(\mathbf{x})) \right\} d\mathbf{x} \geq 0. \quad (5)$$

Using this inequality, we propose the following empirical risk with the non-negative correction:

$$\widehat{\text{nnBR}}_f(r) := \hat{\mathbb{E}}_{\text{nu}}[\ell_2(r(X))] + \left( \hat{\mathbb{E}}_{\text{de}}[\ell_1(r(X))] - C\hat{\mathbb{E}}_{\text{nu}}[\ell_1(r(X))] \right)_+, \quad (6)$$

where  $(\cdot)_+ := \max\{0, \cdot\}$ . Our *Deep direct DRE* (D3RE) is based on minimizing  $\widehat{\text{nnBR}}_f(r)$ .

**Remark 1** (Choice of  $C$ ). In practice, selecting the hyper-parameter  $C$  does not require accurate knowledge of  $\bar{R}$  because any  $0 < C < 1/\bar{R}$  is sufficient to justify the non-negative correction. However, selecting  $C$  that is too small may damage the empirical performance. See Section 5.2.

**nnBR Divergence with Existing Methods:** The above strategy can be instantiated in various methods previously proposed for DRE. Here, we introduce the empirical risks under nnBR divergence, which correspond to LSIF, UKL, BKL, and PULogLoss as follows:

$$\begin{aligned} \widehat{\text{nnBR}}_{\text{LSIF}}(r) &:= -\hat{\mathbb{E}}_{\text{nu}} \left[ r(X) - \frac{C}{2} r^2(X) \right] + \left( \frac{1}{2} \hat{\mathbb{E}}_{\text{de}} [r^2(X)] - \frac{C}{2} \hat{\mathbb{E}}_{\text{nu}} [r^2(X)] \right)_+, \\ \widehat{\text{nnBR}}_{\text{UKL}}(r) &= -\hat{\mathbb{E}}_{\text{nu}} [\log(r(X)) - Cr(X)] + \left( \hat{\mathbb{E}}_{\text{de}} [r(X)] - C\hat{\mathbb{E}}_{\text{nu}} [r(X)] \right)_+, \\ \widehat{\text{nnBR}}_{\text{BKL}}(r) &= -\hat{\mathbb{E}}_{\text{nu}} \left[ \log \left( \frac{r(X)}{1+r(X)} \right) + C \log \left( \frac{1}{1+r(X)} \right) \right] \\ &\quad + \left( -\hat{\mathbb{E}}_{\text{de}} \left[ \log \left( \frac{1}{1+r(X)} \right) \right] + C\hat{\mathbb{E}}_{\text{nu}} \left[ \log \left( \frac{1}{1+r(X)} \right) \right] \right)_+, \\ \widehat{\text{nnBR}}_{\text{PU}}(r) &:= -C\hat{\mathbb{E}}_{\text{nu}} [\log(r(X))] + \left( C\hat{\mathbb{E}}_{\text{nu}} [\log(1-r(X))] - \hat{\mathbb{E}}_{\text{de}} [\log(1-r(X))] \right)_+. \end{aligned}$$

More detailed derivation of  $\tilde{f}$  is in Appendix B. In practice, using flexible models for KLIEP poses another problem that the constrained optimization is no longer convex and is difficult to solve. Therefore, we experiment with UKL, unconstrained minimization of the objective function of KLIEP. In Appendix C, we provide the pseudo code of D3RE. For improving the performance heuristically, we use gradient ascending.

## 4 Theoretical Justification of D3RE

In this section, we confirm the validity of the proposed method by providing an estimation error bound. Given  $n \in \mathbb{N}$  and a distribution  $p$ , we define the *Rademacher complexity*  $\mathcal{R}_n^p$  of a function class  $\mathcal{H}$  as  $\mathcal{R}_n^p(\mathcal{H}) := \mathbb{E}_p \mathbb{E}_\sigma \left[ \sup_{r \in \mathcal{H}} \left| \frac{1}{n} \sum_{i=1}^n \sigma_i r(X_i) \right| \right]$ , where  $\{\sigma_i\}_{i=1}^n$  are independent uniform sign variables. For simplicity, we omit  $r^*$  from the notation of  $\text{BR}_f$  when there is no ambiguity.

#### 4.1 Estimation Error Bound based on Rademacher Complexity

The following theorem provides an estimation error bound in terms of  $\mathcal{R}_n^p$ . Here, we state a special case of Theorem 2 in Appendix H such that the *consistent correction function* is  $(\cdot)_+$ .

**Assumption 3.** Let  $I_r := (b_r, B_r)$ . Assume that there exists an empirical risk minimizer  $\hat{r} \in \arg \min_{r \in \mathcal{H}} \widehat{\text{nnBR}}_f(r)$  and a population risk minimizer  $\bar{r} \in \arg \min_{r \in \mathcal{H}} \text{BR}_f(r)$ . Assume  $B_\ell := \sup_{t \in I_r} \{\max\{|\ell_1(t)|, |\ell_2(t)|\}\} < \infty$ . Also assume  $\ell_1$  (resp.  $\ell_2$ ) is  $L_{\ell_1}$ -Lipschitz (resp.  $L_{\ell_2}$ -Lipschitz) on  $I_r$ . Assume also that  $\inf_{r \in \mathcal{H}} (\mathbb{E}_{\text{de}} - C\mathbb{E}_{\text{nu}})\ell_1(r(X)) > 0$  holds.

**Theorem 1** (Estimation error bound). *Under Assumption 3, for any  $\delta \in (0, 1)$ , with probability at least  $1 - \delta$ , we have*

$$\text{BR}_f(\hat{r}) - \text{BR}_f(\bar{r}) \leq L_{\ell_1} \mathcal{R}_{n_{\text{de}}}^{p_{\text{de}}}(\mathcal{H}) + 8(CL_{\ell_1} + L_{\ell_2})\mathcal{R}_{n_{\text{nu}}}^{p_{\text{nu}}}(\mathcal{H}) + 2\Phi_C^f(n_{\text{nu}}, n_{\text{de}}) + B_\ell \sqrt{8 \left( \frac{1}{n_{\text{de}}} + \frac{(1+C)^2}{n_{\text{nu}}} \right) \log \frac{1}{\delta}},$$

where  $\Phi_C^f(n_{\text{nu}}, n_{\text{de}}) := (1+C)B_\ell \exp\left(-\frac{2\alpha^2}{(B_\ell^2/n_{\text{de}}) + (C^2 B_\ell^2/n_{\text{nu}})}\right)$  and  $\alpha > 0$  is a constant determined in the proof of Lemma 3 in Appendix H.

In order for the boundedness and Lipschitz continuity in Assumption 3 to hold for the loss functions involving a logarithm (UKL, BKL, PU), a technical assumption  $b_r > 0$  is sufficient. We obtain a theoretical guarantee for D3RE from Theorem 1 by additionally imposing Assumption 4 to bound the Rademacher complexities using a previously known result (Golowich et al., 2019, Theorem 1).

**Assumption 4** (Neural networks with bounded complexity). Assume that  $p_{\text{nu}}$  and  $p_{\text{de}}$  have bounded supports:  $\sup_{x \in \mathcal{X}_{\text{de}}} \|x\| < \infty$ . Also assume that  $\mathcal{H}$  consists of real-valued neural networks of depth  $L$  over the domain  $\mathcal{X}$ , where each parameter matrix  $W_j$  has the Frobenius norm at most  $B_{W_j} \geq 0$  and with 1-Lipschitz activation functions  $\varphi_j$  that are positive-homogeneous (i.e.,  $\varphi_j$  is applied element-wise and  $\varphi_j(\alpha t) = \alpha \varphi_j(t)$  for all  $\alpha \geq 0$ ).

Under Assumption 4, Lemma 4 in Appendix I reveals  $\mathcal{R}_{n_{\text{nu}}}^{p_{\text{nu}}}(\mathcal{H}) = \mathcal{O}(1/\sqrt{n_{\text{nu}}})$  and  $\mathcal{R}_{n_{\text{de}}}^{p_{\text{de}}}(\mathcal{H}) = \mathcal{O}(1/\sqrt{n_{\text{de}}})$ . By combining these with Theorem 1, we obtain the following corollary:

**Corollary 1** (Estimation error bound for D3RE). *Under Assumptions 3 and 4, for any  $\delta \in (0, 1)$ , we have with probability at least  $1 - \delta$ ,*

$$\text{BR}_f(\hat{r}) - \text{BR}_f(\bar{r}) \leq \frac{\kappa_1}{\sqrt{n_{\text{de}}}} + \frac{\kappa_2}{\sqrt{n_{\text{nu}}}} + 2\Phi_C^f(n_{\text{nu}}, n_{\text{de}}) + B_\ell \sqrt{8 \left( \frac{1}{n_{\text{de}}} + \frac{(1+C)^2}{n_{\text{nu}}} \right) \log \frac{1}{\delta}},$$

where  $\kappa_1, \kappa_2$  are constants that depend on  $C, f, B_p, L$ , and  $B_{W_j}$ .

#### 4.2 Estimation Error Bound for $L^2$ Distance

Theorem 1 and Corollary 1 can be readily turned into  $L^2$  distance bounds by applying Lemma 1, which can be more convenient for the theoretical analyses for subsequent tasks relying on the density ratio estimator (Cortes et al., 2008). The proof can be found in Appendix J.

**Lemma 1** (Estimation error bound in  $L^2$  distance). *Let  $\mathcal{H}_2 := \{r : \mathcal{X} \rightarrow I_r \mid \int |r(x)|^2 dx < \infty\}$  and assume the true density ratio  $r^*$  is in  $\mathcal{H}_2$ . If  $\inf_{t \in I_r} f''(t) > 0$ , then there exists  $\mu > 0$  such that  $\|\hat{r} - r^*\|_{L^2(p_{\text{de}})}^2 \leq$*

$$\underbrace{\frac{2}{\mu} (\text{BR}_f(\hat{r}) - \text{BR}_f(\bar{r}))}_{\text{Theorem 1 or Corollary 1}} + \underbrace{\frac{2}{\mu} (\text{BR}_f(\bar{r}) - \text{BR}_f(r^*))}_{\text{Best approximation error}}.$$

Note that the strong-convexity assumption of Lemma 1 could be exploited to investigate the convergence rate in more detail, via finer-grained proof techniques such as local Rademacher complexity. Nevertheless, the above theoretical guarantee already suffices for the basic justification of D3RE.

### 5 Experiment with Image Data

In this section, we experimentally show how the existing estimators fail to estimate the density ratio when using neural networks and that our proposed estimators succeed. To investigate the performances, we consider PU learning. For a binary classification problem with labels  $y \in \{-1, +1\}$ , we consider training a classifier only from  $p(x \mid y = +1)$  and  $p(x)$  to find a positive data point in test data sampled from  $p(x)$ . The goal is to maximize the *area under the receiver operating characteristic* (AUROC) curve, which is a criterion used for anomaly detection, by

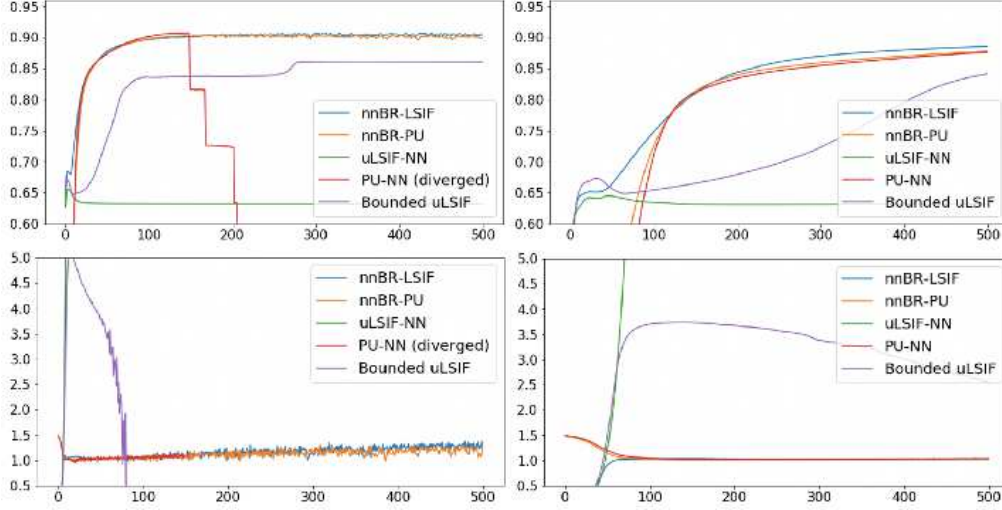


Figure 1: Experimental results of Section 5.1. The horizontal axis is epoch, and the vertical axis is AUROC. The learning rates of the left and right graphs are  $1 \times 10^{-4}$  and  $1 \times 10^{-5}$ , respectively. The upper graphs show the AUROCs and the lower graphs show  $\mathbb{E}_{\text{de}}[\hat{r}(X)]$ , which will approach 1 when we successfully estimate the density ratio.

estimating the density ratio  $r^*(x) = p(x | y = +1)/p(x)$ . We construct the positive and negative dataset from CIFAR-10<sup>1</sup>(Krizhevsky, 2009) dataset with 10 classes. The positive dataset comprises ‘airplane’, ‘automobile’, ‘ship’, and ‘truck’; the negative dataset comprises ‘bird’, ‘cat’, ‘deer’, ‘dog’, ‘frog’, and ‘horse’. We use 1,000 positive data sampled from  $p(x | y = +1)$  and 1,000 unlabeled data sampled from  $p(x)$  to train the models. Then, we calculate the AUROCs using 10,000 test data sampled from  $p(x)$ . In this case, it is desirable to set  $C < \frac{1}{2}$  because

$$\frac{p(x|y=+1)}{0.5p(x|y=+1)+0.5p(x|y=-1)} = \frac{1}{0.5+0.5\frac{p(x|y=-1)}{p(x|y=+1)}}.$$

For demonstrative purposes, we use the CNN architecture from the PyTorch tutorial (Paszke et al., 2019). Details of the network structure are shown in Appendix D.2. The model is trained using Adam without weight decay and the parameters  $(\beta_1, \beta_2, \epsilon)$  in Kingma & Ba (2015) are fixed at the default of PyTorch, namely  $(0.9, 0.999, 10^{-8})$ .

### 5.1 Comparison with Naive Estimators

First, we compare two of the proposed estimators,  $\widehat{\text{nnBR}}_{\text{PU}}$  (nnBR-PU) and  $\widehat{\text{nnBR}}_{\text{LSIF}}$  (nnBR-LSIF), with the existing estimators,  $\widehat{\text{BR}}_{\text{PU}}$  (PU-NN) and  $\widehat{\text{BR}}_{\text{LSIF}}$  (uLSIF-NN). We use the logistic loss for PULogLoss. Additionally, we experiment with uLSIF-NN using a naively capped model  $\tilde{r}(x) = \min\{r(x), 1/C\}$  (bounded uLSIF). We fix the hyperparameter  $C$  at  $1/3$ . We report the results for two learning rates,  $1 \times 10^{-4}$  and  $1 \times 10^{-5}$ . We conducted 10 trials, and calculated the average AUROCs. We also compute  $\hat{\mathbb{E}}_{\text{de}}[\hat{r}(X)]$ , which should be close to 1 if we successfully estimate the density ratio, because  $\int (p(x|y = +1)/p(x))p(x)dx = 1$ . The results are in Figure 1. In all cases, the proposed estimators outperform the other methods. In contrast, the unstable behaviors of PU-NN and LSIF-NN are caused by overfitting (also see (Kiryo et al., 2017) or Appendix F.1).

### 5.2 Empirical Sensitivity Analysis with regard to the Upper Bounds of the Density Ratio

Next, we investigate the sensitivity of D3RE to the hyperparameter  $C$ . We use nnBR-LSIF and nnBR-PU as in Section 5.1, but var the hyperparameter  $C$  in  $\{1/5, 1/2, 2/3\}$ . The other settings remain unchanged from the previous section. These results are shown in Figure 3 in Appendix F.1. For  $\overline{R} = 2.0$ , the estimator show a better performance when  $1/C$  is close to 2.0.

<sup>1</sup>See <https://www.cs.toronto.edu/~kriz/cifar.html>.

Table 2: Average AUROC curve (Mean) with the standard deviation (SD) over 5 trials of anomaly detection methods. For all datasets, each model was trained on a single class and tested against all other classes. The best figure is in bold.

CIFAR-10 Network	uLSIF-NN LeNet		nnBR-LSIF LeNet		nnBR-PU LeNet		nnBR-LSIF WRN		nnBR-PU WRN		Deep SAD LeNet		GT WRN	
Inlier Class	Mean	SD	Mean	SD	Mean	SD	Mean	SD	Mean	SD	Mean	SD	Mean	SD
plane	0.745	0.056	0.934	0.002	<b>0.943</b>	0.001	0.925	0.004	0.923	0.001	0.627	0.066	0.697	0.009
car	0.758	0.078	0.957	0.002	<b>0.968</b>	0.001	0.965	0.002	0.960	0.001	0.606	0.018	0.962	0.003
bird	0.768	0.012	0.850	0.007	<b>0.878</b>	0.004	0.844	0.004	0.858	0.004	0.404	0.006	0.752	0.002
cat	0.745	0.037	0.820	0.003	<b>0.856</b>	0.002	0.810	0.009	0.841	0.002	0.517	0.018	0.727	0.014
deer	0.758	0.036	0.886	0.004	<b>0.909</b>	0.002	0.864	0.008	0.872	0.002	0.704	0.052	0.863	0.014

FMNIST Network	uLSIF-NN LeNet		nnBR-LSIF LeNet		nnBR-PU LeNet		nnBR-LSIF WRN		nnBR-PU WRN		Deep SAD LeNet		GT WRN	
Inlier Class	Mean	SD	Mean	SD	Mean	SD	Mean	SD	Mean	SD	Mean	SD	Mean	SD
T-shirt/top	0.960	0.005	0.981	0.001	<b>0.985</b>	0.000	0.984	0.001	0.982	0.000	0.558	0.031	0.890	0.007
Trouser	0.961	0.010	0.998	0.000	<b>1.000</b>	0.000	0.998	0.000	0.998	0.000	0.758	0.022	0.974	0.004
Pullover	0.944	0.012	0.976	0.001	0.980	0.001	<b>0.983</b>	0.002	0.972	0.001	0.617	0.046	0.902	0.005
Dress	0.973	0.006	0.986	0.001	<b>0.992</b>	0.000	0.991	0.001	0.986	0.000	0.525	0.038	0.843	0.014
Coat	0.958	0.006	0.978	0.001	<b>0.983</b>	0.000	0.981	0.002	0.974	0.000	0.627	0.029	0.885	0.003

### 5.3 Comparison with Various Estimators using nnBR Divergence

Finally, we examine the performances of nnBR-LSIF, nnBR-PU, nnBR-UKL, and nnBR-BKL. The learning rate was  $1 \times 10^{-3}$ , and the other settings were identical to those in the previous experiments. These results are shown in Figure 3 in Appendix F.1. Although nnBR-UKL and nnBR-BKL show better performance in earlier epochs, nnBR-LSIF and nnBR-PU appear more stable.

## 6 Applications

As applications of D3RE, we introduce *inlier-based outlier detection* and *covariate shift adaptation* with experiments using benchmark datasets. Moreover, we introduce other applications in Appendix G. In addition to CIFAR-10, we use MNIST<sup>2</sup> (LeCun et al., 1998), fashion-MNIST<sup>3</sup> (Xiao et al., 2017), and a document dataset of Amazon<sup>4</sup> (Blitzer et al., 2007).

### 6.1 Inlier-based Outlier Detection

Hido et al. (2008, 2011) applied the direct DRE for inlier-based outlier detection: finding outliers in a test set based on a training set consisting only of inliers by using the ratio of training and test data densities as an outlier score. Nam & Sugiyama (2015) and Abe & Sugiyama (2019) proposed using neural networks with DRE for this problem. In relation to the experimental setting of Section 5, the problem setting can be seen as a transductive variant of PU learning (Kato et al., 2019).

**Experiments:** We follow the setting proposed by Golan & El-Yaniv (2018) using MNIST, CIFAR-10, and fashion-MNIST. There are ten classes in each dataset; we use one class as the inlier class and all other classes as the outliers. For example, in the case of CIFAR-10, there are 5,000 train data per class. On the other hand, there are 1,000 test data for each class, which consist of 1,000 inlier samples and 9,000 outlier samples. The AUROC is used as a metric to evaluate whether an outlier class can be detected in the test data. We compare the proposed methods with benchmark methods of deep semi-supervised anomaly detection (DeepSAD) (Ruff et al., 2020) and geometric transformations (GT) (Golan & El-Yaniv, 2018). The details of each method are shown in Appendix E. To compare the methods fairly, we use the same architectures of neural networks from Golan & El-Yaniv (2018) and Ruff et al. (2020), LeNet and Wide Resnet, for D3RE. The details of the structures are shown in Appendix D. A part of the experimental results with CIFAR-10 and fashion-MNIST are shown in Table 2 due to the limitation of the space. The full results are shown in Table 4 in Appendix F.2. The proposed estimators show the better performance than benchmarks.

<sup>2</sup>MNIST has 10 classes from 0 to 9. See <http://yann.lecun.com/exdb/mnist/>.

<sup>3</sup>fashion-MNIST has 10 classes. See <https://github.com/zalandoresearch/fashion-mnist>.

<sup>4</sup><http://john.blitzer.com/software.html>

Table 3: Average PD (Mean) with standard deviation (SD) over 10 trials with different seeds per method. The best performing method in terms of the mean PD is specified by bold face.

Domains (Train → Test)	book → dvd		book → elec		book → kitchen		dvd → elec		dvd → kitchen		elec → kitchen	
DRE method	Mean	SD	Mean	SD	Mean	SD	Mean	SD	Mean	SD	Mean	SD
w/o IW	0.126	0.008	0.174	0.010	0.166	0.009	0.162	0.006	0.146	0.010	0.074	0.005
Kernel uLSIF	0.122	0.009	0.162	0.009	0.159	0.007	0.153	0.006	0.142	0.007	0.068	0.005
Kernel KLIEP	0.130	0.010	0.164	0.009	0.161	0.007	0.154	0.006	0.143	0.006	0.070	0.005
uLSIF-NN	0.126	0.008	0.174	0.010	0.166	0.009	0.162	0.006	0.146	0.010	0.074	0.005
PU-NN	0.126	0.008	0.174	0.010	0.166	0.009	0.162	0.006	0.146	0.010	0.074	0.005
nnBR-LSIF	0.120	0.008	<b>0.160</b>	0.008	0.157	0.008	<b>0.148</b>	0.006	<b>0.138</b>	0.007	<b>0.066</b>	0.005
nnBR-PU	<b>0.119</b>	0.008	<b>0.16</b>	0.008	<b>0.156</b>	0.007	<b>0.148</b>	0.005	<b>0.138</b>	0.007	<b>0.066</b>	0.005

## 6.2 Covariate Shift Adaptation by Importance Weighting

*Covariate shift* is a problem that the training input distribution is different from the test input distribution for which we want to make accurate predictions (Bickel et al., 2009; Shimodaira, 2000). To solve this problem, the density ratio has been used via importance weighting (Shimodaira, 2000; Yamada et al., 2010; Reddi et al., 2015).

**Experiments:** We use the Amazon review dataset for multi-domain sentiment analysis (Blitzer et al., 2007). This data consists of text reviews from four different product domains: book, electronics (elec), dvd, and kitchen. Following Chen et al. (2012) and Menon & Ong (2016), we transform the text data using TF-IDF to map them into the instance space  $\mathcal{X} = \mathbb{R}^{10000}$  (Salton & McGill, 1986). Each review is endowed with four labels indicating the positivity of the review, and our goal is to conduct regression for these labels. To achieve this goal, we perform kernel ridge regression with the linear kernel, the Gaussian kernel, and the polynomial kernel, which are denoted by LinearRidge, GaussRidge, and PolyRidge, respectively. We compare results without importance weighting (w/o IW) with results using the density ratio estimated by PU-NN, uLSIF-NN, nnBR-LSIF, nnBR-PU, uLSIF with a linear-in-parameter model and Gaussian kernels (Kernel uLSIF), and KLIEP with a linear-in-parameter model and Gaussian kernels (Kernel KLIEP). We conduct experiments on 2,000 samples from one domain, and test 2,000 samples. Following Menon & Ong (2016), we reduce the dimension into 100 dimensions by principal component analysis when using Kernel uLSIF, Kernel KLEIP, and regressions. Following Menon & Ong (2016) and Cortes & Mohri (2011), the mean and standard deviation of the pairwise disagreement (PD),  $1 - \text{AUROC}$ , is reported. A part of results using PolyRidge is in Table 3. The full results are in Appendix F.3. The methods with D3RE show preferable performance.

## 7 Conclusion

In this paper, we proposed a non-negative correction to the empirical BR divergence for DRE. By using the prior knowledge of the upper bound of the density ratio, we can prevent the overfitting when using flexible models. In our theoretical analysis, we showed the generalization bound of the algorithm. A future direction is to apply D3RE to computer vision and natural language processing.

## Broader Impact

This paper addresses the conventional problem of DRE with neural networks. In general, DRE has the potential to improve various tasks such as anomaly detection, regression under covariate shift, and change point detection. Therefore, this paper has an impact on such fields broadly and also shares the negative outcomes of these fields. For example, the methods for anomaly detection can be applied for the control of people by authorities. On the other hand, these problems are the existing concerns of these fields before we propose the method of this paper. Thus, while the proposed method improves the existing method, it also enlarges the negative points. Negative issues in those fields are not limited to this paper, and discussion from a broader perspective is needed in the future.

## Acknowledgement

TT was supported by Masason Foundation.

## References

Abe, M. and Sugiyama, M. Anomaly detection by deep direct density ratio estimation. *openreview*, 2019.



- Adams, R. P. Bayesian online changepoint detection. Technical report, 2007.
- Ali, S. M. and Silvey, S. D. A general class of coefficients of divergence of one distribution from another. *Journal of the Royal Statistical Society, Series B*(28):131–142, 1966.
- Athey, S. and Wager, S. Efficient policy learning. *arXiv preprint arXiv:1702.02896*, 2017.
- Bartlett, P. L. and Mendelson, S. Rademacher and Gaussian complexities: Risk bounds and structural results. In *Computational Learning Theory*, volume 2111, pp. 224–240. Springer Berlin Heidelberg, 2001.
- Basseville, M. and Nikiforov, I. V. *Detection of abrupt changes: theory and application*. Prentice Hall information and system sciences. Prentice Hall, 1993.
- Bengio, Y., Ducharme, R., and Vincent, P. A neural probabilistic language model. In *NeurIPS*, pp. 932–938. MIT Press, 2001.
- Beygelzimer, A. and Langford, J. The offset tree for learning with partial labels. In *KDD*, pp. 129–138, 2009.
- Bibaut, A., Malenica, I., Vlassis, N., and Van Der Laan, M. More efficient off-policy evaluation through regularized targeted learning. In *ICML*. PMLR, 2019.
- Bickel, S., Brückner, M., and Scheffer, T. Discriminative learning under covariate shift. *J. Mach. Learn. Res.*, 10: 2137–2155, December 2009. ISSN 1532-4435.
- Blitzer, J., Dredze, M., and Pereira, F. Biographies, Bollywood, boom-boxes and blenders: Domain adaptation for sentiment classification. In *Proceedings of the 45th Annual Meeting of the Association of Computational Linguistics*, June 2007.
- Bregman, L. The relaxation method of finding the common point of convex sets and its application to the solution of problems in convex programming. *USSR Computational Mathematics and Mathematical Physics*, 7(3):200 – 217, 1967. ISSN 0041-5553.
- Brodsky, E. and Darkhovsky, B. *Nonparametric Methods in Change Point Problems*. Mathematics and Its Applications. Springer Netherlands, 1993.
- Chen, M., Xu, Z., Weinberger, K. Q., and Sha, F. Marginalized denoising autoencoders for domain adaptation. In *ICML, ICML’12*, pp. 1627–1634, Madison, WI, USA, 2012. Omnipress.
- Cheng, k.-F. and Chu, C. Semiparametric density estimation under a two-sample density ratio model. *Bernoulli*, 10, 08 2004.
- Cole, S. R. and Stuart, E. A. Generalizing evidence from randomized clinical trials to target populations. *American Journal of Epidemiology*, 172(1):107–115, 2010.
- Cortes, C. and Mohri, M. Domain adaptation in regression. In *Algorithmic Learning Theory*, pp. 308–323, Berlin, Heidelberg, 2011. Springer Berlin Heidelberg.
- Cortes, C., Mohri, M., Riley, M., and Rostamizadeh, A. Sample Selection Bias Correction Theory. In *Algorithmic Learning Theory*, pp. 38–53, Berlin, Heidelberg, 2008. Springer.
- Csiszár, I. Information-type measures of difference of probability distributions and indirect observation. *Studia Scientiarum Mathematicarum Hungarica*, (2):229–318, 1967.
- du Plessis, M. C., Niu, G., and Sugiyama, M. Convex formulation for learning from positive and unlabeled data. In *ICML*, pp. 1386–1394, 2015.
- Dudík, M., Langford, J., and Li, L. Doubly Robust Policy Evaluation and Learning. In *ICML*, pp. 1097–1104, 2011.
- Elkan, C. and Noto, K. Learning classifiers from only positive and unlabeled data. In *ICDM*, pp. 213–220, 2008.
- Garnett, R., Osborne, M. A., and Roberts, S. J. Sequential bayesian prediction in the presence of changepoints. In *ICML*, pp. 345–352, New York, NY, USA, 2009. Association for Computing Machinery.
- Golan, I. and El-Yaniv, R. Deep anomaly detection using geometric transformations. In *NeurIPS*, pp. 9758–9769. Curran Associates, Inc., 2018.
- Golowich, N., Rakhlin, A., and Shamir, O. Size-Independent Sample Complexity of Neural Networks. *arXiv:1712.06541 [cs, stat]*, November 2019.
- Goodfellow, I., Pouget-Abadie, J., Mirza, M., Xu, B., Warde-Farley, D., Ozair, S., Courville, A., and Bengio, Y. Generative adversarial nets. In *NeurIPS*, pp. 2672–2680. Curran Associates, Inc., 2014.
- Gretton, A., Smola, A., Huang, J., Schmittfull, M., Borgwardt, K., Schölkopf, B., Candela, J., Sugiyama, M., Schwaighofer, A., and Lawrence, N. Covariate shift by kernel mean matching. *Dataset Shift in Machine Learning*, 131-160 (2009), 01 2009.

- Gustafsson, M. G. L. Surpassing the lateral resolution limit by a factor of two using structured illumination microscopy. *Journal of Microscopy*, 198(2):82–87, 2000.
- Hastie, T., Tibshirani, R., and Friedman, J. *The elements of statistical learning: data mining, inference and prediction*. Springer, 2001.
- Hellinger, E. Neue begründung der theorie quadratischer formen von unendlichvielen veränderlichen. *Journal für die reine und angewandte Mathematik*, 136:210–271, 1909.
- Hido, S., Tsuboi, Y., Kashima, H., Sugiyama, M., and Kanamori, T. Inlier-based outlier detection via direct density ratio estimation. pp. 223–232, 12 2008.
- Hido, S., Tsuboi, Y., Kashima, H., Sugiyama, M., and Kanamori, T. Statistical outlier detection using direct density ratio estimation. *Knowledge and Information Systems*, 26(2):309–336, Feb 2011.
- Huang, J., Gretton, A., Borgwardt, K., Schölkopf, B., and Smola, A. J. Correcting sample selection bias by unlabeled data. In *NeurIPS*, pp. 601–608. MIT Press, 2007.
- Ioffe, S. and Szegedy, C. Batch normalization: Accelerating deep network training by reducing internal covariate shift. In *ICML*, pp. 448–456, 2015.
- Kaiming He, Xiangyu Zhang, S. R. and Sun, J. Deep residual learning for image recognition. In *CoRR*, 2015.
- Kallus, N. and Uehara, M. Intrinsically efficient, stable, and bounded off-policy evaluation for reinforcement learning. In *NeurIPS*, pp. 3320–3329. 2019.
- Kanamori, T., Hido, S., and Sugiyama, M. A least-squares approach to direct importance estimation. *Journal of Machine Learning Research*, 10(Jul.):1391–1445, 2009.
- Kanamori, T., Suzuki, T., and Sugiyama, M. f-divergence estimation and two-sample homogeneity test under semi-parametric density-ratio models. *IEEE Transactions on Information Theory*, 58, 10 2010.
- Kanamori, T., Suzuki, T., and Sugiyama, M. Statistical analysis of kernel-based least-squares density-ratio estimation. *Mach. Learn.*, 86(3):335–367, March 2012. ISSN 0885-6125.
- Kato, M. Identifying different definitions of future in the assessment of future economic conditions: Application of pu learning and text mining. *arXiv*, 2019.
- Kato, M., Teshima, T., and Honda, J. Learning from positive and unlabeled data with a selection bias. In *ICLR*, 2019.
- Kato, M., Uehara, M., and Yasui, S. Off-policy evaluation and learning for external validity under a covariate shift, 2020.
- Kawahara, Y. and Sugiyama, M. Change-point detection in time-series data by direct density-ratio estimation. In *ICDM*, 2009.
- Keziou, A. Utilisation des divergences entre mesures en statistique inferentielle. *PhD thesis*, 2003.
- Keziou, A. and Leoni-Aubin, S. Test of homogeneity in semiparametric two-sample density ratio models. *Comptes Rendus Mathématique - C R MATH*, 340:905–910, 06 2005.
- Kingma, D. P. and Ba, J. Adam: A method for stochastic optimization. In *ICLR*, 2015.
- Kiryo, R., Niu, G., du Plessis, M. C., and Sugiyama, M. Positive-unlabeled learning with non-negative risk estimator. *arXiv:1703.00593 [cs, stat]*, 2017.
- Krizhevsky, A. Learning multiple layers of features from tiny images. 2009.
- Krizhevsky, A., Sutskever, I., and Hinton, G. E. Imagenet classification with deep convolutional neural networks. In *NeurIPS*, pp. 1097–1105. Curran Associates, Inc., 2012.
- Kullback, S. and Leibler, R. A. On information and sufficiency. *Ann. Math. Statist.*, 22(1):79–86, 1951.
- LeCun, Y., Bottou, L., Bengio, Y., and Haffner, P. Gradient-based learning applied to document recognition. In *Proceedings of the IEEE*, volume 86, pp. 2278–2324, 1998.
- Ledoux, M. and Talagrand, M. *Probability in Banach Spaces: Isoperimetry and Processes*. Springer, Berlin, 1991.
- Li, L., Chu, W., Langford, J., and Schapire, R. E. A contextual-bandit approach to personalized news article recommendation. In *WWW*, pp. 661–670, 2010.
- Liu, S., Yamada, M., Collier, N., and Sugiyama, M. Change-point detection in time-series data by relative density-ratio estimation. In *Structural, Syntactic, and Statistical Pattern Recognition*, pp. 363–372, Berlin, Heidelberg, 2012. Springer Berlin Heidelberg.
- Loevinger, J. The technic of homogeneous tests compared with some aspects of "scale analysis" and factor analysis. *Psychological Bulletin*, 45(6):507–529, 1948. ISSN 0033-2909.

- Lu, N., Zhang, T., Niu, G., and Sugiyama, M. Mitigating overfitting in supervised classification from two unlabeled datasets: A consistent risk correction approach. *arXiv:1910.08974 [cs, stat]*, March 2020.
- McDiarmid, C. On the method of bounded differences. In *Surveys in Combinatorics, 1989: Invited Papers at the Twelfth British Combinatorial Conference*, London Mathematical Society Lecture Note Series, pp. 148–188. Cambridge University Press, 1989.
- Menon, A. and Ong, C. S. Linking losses for density ratio and class-probability estimation. In *ICML*, volume 48, pp. 304–313, New York, New York, USA, 2016.
- Mohri, M., Rostamizadeh, A., and Talwalkar, A. *Foundations of Machine Learning*. Adaptive Computation and Machine Learning. The MIT Press, Cambridge, Massachusetts, second edition, 2018.
- Nam, H. and Sugiyama, M. Direct density ratio estimation with convolutional neural networks with application in outlier detection. *IEICE Transactions on Information and Systems*, E98.D(5):1073–1079, 2015.
- Narita, Y., Yasui, S., and Yata, K. Efficient counterfactual learning from bandit feedback. *AAAI*, 2019.
- Nguyen, M. N., Li, X.-L., and Ng, S.-K. Positive unlabeled learning for time series classification. In *IJCAI*, pp. 1421–1426, 2011.
- Niu, G., du Plessis, M. C., Sakai, T., Ma, Y., and Sugiyama, M. Theoretical comparisons of positive-unlabeled learning against positive-negative learning. In *NeurIPS*, pp. 1199–1207, 2016.
- Nowozin, S., Cseke, B., and Tomioka, R. f-gan: Training generative neural samplers using variational divergence minimization. In *NeurIPS*, pp. 271–279. Curran Associates, Inc., 2016.
- Oberst, M. and Sontag, D. Counterfactual off-policy evaluation with gumbel-max structural causal models. In *ICML*, volume 97, pp. 4881–4890, 2019.
- Paquet, U. Empirical bayesian change point detection. *Graphical Models*, 1995, 01 2007.
- Paszke, A., Gross, S., Massa, F., Lerer, A., Bradbury, J., Chanan, G., Killeen, T., Lin, Z., Gimelshein, N., Antiga, L., Desmaison, A., Kopf, A., Yang, E., DeVito, Z., Raison, M., Tejani, A., Chilamkurthy, S., Steiner, B., Fang, L., Bai, J., and Chintala, S. Pytorch: An imperative style, high-performance deep learning library. In *NeurIPS*, pp. 8024–8035. Curran Associates, Inc., 2019.
- Pearl, J. and Bareinboim, E. External validity: From do-calculus to transportability across populations. *Statistical Science*, 29, 2014.
- Pearson, K. On the criterion that a given system of deviations from the probable in the case of a correlated system of variables is such that it can reasonably be supposed to have arisen from random sampling. *Philosophical Magazine*, 5(50):157–175, 1900.
- Qin, J. Inferences for case-control and semiparametric two-sample density ratio models. *Biometrika*, 85(3):619–630, 1998.
- Reddi, S. J., Póczos, B., and Smola, A. J. Doubly robust covariate shift correction. In *AAAI*, pp. 2949–2955. AAAI Press, 2015.
- Ruff, L., Vandermeulen, R. A., Görnitz, N., Binder, A., Müller, E., Müller, K.-R., and Kloft, M. Deep semi-supervised anomaly detection. In *ICLR*, 2020.
- Salton, G. and McGill, M. J. Introduction to modern information retrieval. 1986.
- Shimodaira, H. Improving predictive inference under covariate shift by weighting the log-likelihood function. *Journal of statistical planning and inference*, 90(2):227–244, 2000.
- Smola, A., Song, L., and Teo, C. H. Relative novelty detection. In *AISTATS*, volume 5 of *Proceedings of Machine Learning Research*, pp. 536–543, Hilton Clearwater Beach Resort, Clearwater Beach, Florida USA, 2009. PMLR.
- Springenberg, J., Dosovitskiy, A., Brox, T., and Riedmiller, M. Striving for simplicity: The all convolutional net. In *ICLR (workshop track)*, 2015.
- Sugiyama, M., Suzuki, T., Nakajima, S., Kashima, H., von Büna, P., and Kawanabe, M. Direct importance estimation for covariate shift adaptation. *Annals of the Institute of Statistical Mathematics*, 60:699–746, 02 2008.
- Sugiyama, M., Kanamori, T., Suzuki, T., Hido, S., Sese, J., Takeuchi, I., and Wang, L. A density-ratio framework for statistical data processing. *IPSJ Transactions on Computer Vision and Applications*, 1:183–208, 2009.
- Sugiyama, M., Suzuki, T., Itoh, Y., Kanamori, T., and Kimura, M. Least-squares two-sample test. *Neural networks : the official journal of the International Neural Network Society*, 24:735–51, 04 2011a.
- Sugiyama, M., Suzuki, T., and Kanamori, T. Density ratio matching under the bregman divergence: A unified framework of density ratio estimation. *Annals of the Institute of Statistical Mathematics*, 64, 10 2011b.

- Sugiyama, M., Suzuki, T., and Kanamori, T. *Density Ratio Estimation in Machine Learning*. Cambridge University Press, New York, NY, USA, 1st edition, 2012.
- Uehara, M., Sato, I., Suzuki, M., Nakayama, K., and Matsuo, Y. Generative adversarial tests from a density ratio estimation perspective. 2016. URL <https://arxiv.org/abs/1610.02920>.
- Vapnik, V. N. *Statistical Learning Theory*. Wiley, September 1998.
- Wang, Y.-X., Agarwal, A., and Dudik, M. Optimal and adaptive off-policy evaluation in contextual bandits. In *ICML*, pp. 3589–3597, 2017.
- Xiao, H., Rasul, K., and Vollgraf, R. Fashion-mnist: a novel image dataset for benchmarking machine learning algorithms. *ArXiv*, abs/1708.07747, 2017.
- Yamada, M., Sugiyama, M., Wichern, G., and Simm, J. Direct importance estimation with a mixture of probabilistic principal component analyzers. *IEICE Transactions*, 93-D:2846–2849, 10 2010.
- Yamanishi, K. and Takeuchi, J. A unifying framework for detecting outliers and change points from non-stationary time series data. pp. 676–681, 12 2002.
- Zagoruyko, S. and Komodakis, N. Wide residual networks. In *Proceedings of the British Machine Vision Conference (BMVC)*, pp. 87.1–87.12. BMVA Press, September 2016.

## A Details of Existing Methods for DRE

In this section, we overview examples of DRE methods in the framework of the density ratio matching under BR divergence.

**Least Squares Importance Fitting (LSIF):** LSIF minimizes the squared error between a density ratio model  $r$  and the true density ratio  $r^*$  defined as follows (Kanamori et al., 2009):

$$R_{\text{LSIF}}(r) = \mathbb{E}_{\text{de}}[(r(X) - r^*(X))^2] = \mathbb{E}_{\text{de}}[(r^*(X))^2] - 2\mathbb{E}_{\text{nu}}[r(X)] + \mathbb{E}_{\text{de}}[(r(X))^2].$$

In the *unconstrained LSIF* (uLSIF) (Kanamori et al., 2009), we ignore the first term in the above equation and estimate the density ratio by the following minimization problem:

$$\hat{r} = \arg \min_{r \in \mathcal{H}} \left[ \frac{1}{2} \hat{\mathbb{E}}_{\text{de}}[(r(X))^2] - \hat{\mathbb{E}}_{\text{nu}}[r(X)] + \mathcal{R}(r) \right], \quad (7)$$

where  $\mathcal{R}$  is a regularization term. This empirical risk minimization is equal to minimizing the empirical BR divergence defined in (3) with  $f(t) = (t - 1)^2/2$ .

**Unnormalized Kullback–Leibler (UKL) Divergence and KL Importance Estimation Procedure (KLIEP):** The KL importance estimation procedure (KLIEP) is derived from the unnormalized Kullback–Leibler (UKL) divergence objective (Sugiyama et al., 2011b), which uses  $f(t) = t \log(t) - t$ . Ignoring the terms which are irrelevant for the optimization, we obtain the unnormalized Kullback–Leibler (UKL) divergence objective (Sugiyama et al., 2011b) as

$$\text{BR}_{\text{UKL}}(r) = \mathbb{E}_{\text{de}}[r(X)] - \mathbb{E}_{\text{nu}}[\log(r(\mathbf{x}))].$$

KLIEP further imposes a constraint that the ratio model  $r(\mathbf{x})$  is non-negative for all  $\mathbf{x}$  and is normalized as

$$\hat{\mathbb{E}}_{\text{de}}[r(X)] = 1.$$

Then, following is the optimization criterion of KLIEP (Sugiyama et al., 2008):

$$\begin{aligned} & \max_r \hat{\mathbb{E}}_{\text{nu}}[\log(r(\mathbf{x}))] \\ & \text{s.t. } \hat{\mathbb{E}}_{\text{de}}[r(X)] = 1 \text{ and } r(\mathbf{x}) \geq 0 \text{ for all } \mathbf{x}. \end{aligned}$$

**Logistic Regression:** By using  $f(t) = \log(t) - (1 + t) \log(1 + t)$ , we obtain the following BR divergence called the binary Kullback–Leibler (BKL) divergence:

$$\text{BR}_{\text{BKL}}(r) = -\mathbb{E}_{\text{de}} \left[ \log \left( \frac{1}{1 + r(X)} \right) \right] - \mathbb{E}_{\text{nu}} \left[ \log \left( \frac{r(X)}{1 + r(\mathbf{x})} \right) \right].$$

This BR divergence is derived from a formulation based on the logistic regression (Hastie et al., 2001; Sugiyama et al., 2011b).

**PU Learning with the Log Loss:** Consider a binary classification problem and let  $\mathbf{x}$  and  $y \in \{\pm 1\}$  be the feature and the label of a sample, respectively. In PU learning, the goal is to train a classifier only using positive data sampled from  $p(\mathbf{x} \mid y = +1)$ , and unlabeled data sampled from  $p(\mathbf{x})$  in binary classification (Elkan & Noto, 2008). More precisely, this problem setting of PU learning is called the *case-control scenario* (Elkan & Noto, 2008; Niu et al., 2016). Let  $\mathcal{G}$  be the set of measurable functions from  $\mathcal{X}$  to  $[\epsilon, 1 - \epsilon]$ , where  $\epsilon \in (0, 1/2)$  is a small positive value. For a loss function  $\ell : \mathbb{R} \times \{\pm 1\} \rightarrow \mathbb{R}^+$ , du Plessis et al. (2015) showed that the classification risk of  $g \in \mathcal{G}$  in the PU problem setting can be expressed as

$$R_{\text{PU}}(g) = \pi \int (\ell(g(X), +1) - \ell(g(X), -1)) p(\mathbf{x} \mid y = +1) d\mathbf{x} + \int \ell(g(X), -1) p(\mathbf{x}) d\mathbf{x}. \quad (8)$$

According to Kato et al. (2019), we can derive the following risk for DRE from the risk for PU learning (8) as follows:

$$\text{BR}_{\text{PU}}(g) = \frac{1}{R} \mathbb{E}_{\text{nu}}[-\log(g(X)) + \log(1 - g(X))] - \mathbb{E}_{\text{de}}[\log(1 - g(X))],$$

and Kato et al. (2019) showed that  $g^* = \arg \min_{g \in \mathcal{G}} \text{BR}_{\text{PU}}(g)$  satisfies the following:

**Proposition 1.** It holds almost everywhere that

$$g^*(\mathbf{x}) = \begin{cases} 1 - \varepsilon & (\mathbf{x} \notin D_2), \\ C \frac{p_{\text{nu}}(\mathbf{x})}{p_{\text{de}}(\mathbf{x})} & (\mathbf{x} \in D_1 \cap D_2), \\ \varepsilon & (\mathbf{x} \notin D_1), \end{cases}$$

where  $C = \frac{1}{R}$ ,  $D_1 = \{\mathbf{x} \mid Cp_{\text{nu}}(\mathbf{x}) \geq \varepsilon p_{\text{de}}(\mathbf{x})\}$ , and  $D_2 = \{\mathbf{x} \mid Cp_{\text{nu}}(\mathbf{x}) \leq (1 - \varepsilon)p_{\text{de}}(\mathbf{x})\}$ .

Using this result, we define the empirical version of  $\text{BR}_{\text{PU}}(g)$  as follows:

$$\widehat{\text{BR}}_{\text{PU}}(r^* \| r) := C \mathbb{E}_{\text{nu}} [-\log(r(\mathbf{x}_i)) + \log(1 - r(\mathbf{x}_j))] - \mathbb{E}_{\text{de}} [\log(1 - r(\mathbf{x}_i))].$$

**Remark 2** (DRE and PU learning). Menon & Ong (2016) showed that minimizing a proper CPE loss is equivalent to minimizing a BR divergence to the true density ratio, and demonstrated the viability of using existing losses from one problem for the other for CPE and DRE. Kato et al. (2019) pointed out the relation between the PU learning and density ratio estimation and leveraged it to solve a sample selection bias problem in PU learning. In this paper, we introduced the BR divergence with  $f(t) = \log(1 - Ct) + Ct(\log(Ct) - \log(1 - Ct))$ , inspired by the objective function of PU learning with the log loss. In the terminology of Menon & Ong (2016), this  $f$  results in a DRE objective without a *link function*. In other words, it yields a direct DRE method.

## B Examples of $\tilde{f}$

Here, we show the examples of  $\tilde{f}$  such that  $\partial f(t) = C(\partial f(t)t - f(t)) + \tilde{f}(t)$ , where  $\tilde{f}(t)$  is bounded from above, and  $\partial f(t)t - f(t)$  is non-negative.

First, we consider  $f(t) = (t - 1)^2/2$ , which results in the LSIF objective. Because  $\partial f(t) = t - 1$ , we have

$$\begin{aligned} t - 1 &= C((t - 1)t - (t - 1)^2/2) + \tilde{f}(t) \\ \Leftrightarrow \tilde{f}(t) &= -C((t - 1)t - (t - 1)^2/2) + t - 1 = -\frac{C}{2}t^2 + \frac{C}{2} + t - 1. \end{aligned}$$

The function is a concave quadratic function, therefore it is upper bounded.

Second, we consider  $f(t) = t \log(t) - t$ , which results in the UKL or KLIEP objective. Because  $\partial f(t) = \log(t)$ , we have

$$\begin{aligned} \log(t) &= C(\log(t)t - t \log(t) + t) + \tilde{f}(t) \\ \Leftrightarrow \tilde{f}(t) &= -tC + \log(t). \end{aligned}$$

We can easily confirm that the function is upper bounded by taking the derivative and finding that  $t = 1/C$  gives the maximum.

Third, we consider  $f(t) = t \log(t) - (1 + t) \log(1 + t)$ , which is used for DRE based on LR or BKL. Because  $\partial f(t) = \log(t) - \log(1 + t)$ , we have

$$\begin{aligned} \log(t) - \log(1 + t) &= C((\log(t) - \log(1 + t))t - t \log(t) + (1 + t) \log(1 + t)) + \tilde{f}(t) \\ \Leftrightarrow \tilde{f}(t) &= -C(\log(1 + t)) + \log(t) - \log(1 + t) = \log\left(\frac{C}{1 + t}\right) + \log\left(\frac{t}{1 + t}\right). \end{aligned}$$

We can easily confirm that the function is upper bounded as the terms involving  $t$  always add up to be negative.

Fourth, we consider the  $f(t)$  in DRE based on PULog. In this case, we can obtain the same risk functional introduced in Kiryo et al. (2017).

## C Implementation

The algorithm for D3RE is described in Algorithm 1. For training with a large amount of data, we adopt the *stochastic optimization* by splitting the dataset into mini-batches. In stochastic optimization, we separate the samples into  $N$  mini-batches as  $(\{\mathbf{x}_i^{\text{nu}}\}_{i=1}^{n_{\text{nu},j}}, \{\mathbf{x}_i^{\text{de}}\}_{i=1}^{n_{\text{de},j}})$  ( $j = 1, \dots, N$ , where  $n_{\text{nu},j}$  and  $n_{\text{de},j}$  are the sample sizes in each mini-batch. Then, we consider taking sample average in each mini-batch. Let  $\hat{\mathbb{E}}_{\text{nu}}^j$  and  $\hat{\mathbb{E}}_{\text{de}}^j$  be sample averages over  $\{\mathbf{x}_i^{\text{nu}}\}_{i=1}^{n_{\text{nu},j}}$  and  $\{\mathbf{x}_i^{\text{de}}\}_{i=1}^{n_{\text{de},j}}$ . In addition, we use regularization such as L1 and L2 penalties, denoted by  $\mathcal{R}(r)$ . For improving the performance, we heuristically employ *gradient ascent* from Kiryo et al. (2017) when  $\hat{\mathbb{E}}_{\text{de}}[\ell_1(r(X))] - C\hat{\mathbb{E}}_{\text{nu}}[\ell_1(r(X))]$  becomes less than 0, i.e., update the model in the direction that increases the term.

---

**Algorithm 1** D3RE

---

**Input:** Training data  $\{\mathbf{x}_i^{\text{nu}}\}_{i=1}^{n_{\text{nu}}}$  and  $\{\mathbf{x}_i^{\text{de}}\}_{i=1}^{n_{\text{de}}}$ , the algorithm for stochastic optimization such as Adam (Kingma & Ba, 2015), the learning rate  $\gamma$ , the regularization coefficient  $\lambda$ .  
**Output:** A density ratio estimator  $\hat{r}$ .  
**while** No stopping criterion has been met: **do**  
    Create  $N$  mini-batches  $\{(\{\mathbf{x}_i^{\text{nu}}\}_{i=1}^{n_{\text{nu},j}}, \{\mathbf{x}_i^{\text{de}}\}_{i=1}^{n_{\text{de},j}})\}_{j=1}^N$ .  
    **for**  $i = 1$  to  $N$  **do**  
        **if**  $\hat{\mathbb{E}}_{\text{de}}[\ell_1(r(X))] - C\hat{\mathbb{E}}_{\text{nu}}[\ell_1(r(X))] \geq 0$ : **then**  
            Gradient decent: set gradient  $\nabla_r \{\hat{\mathbb{E}}_{\text{nu}}^j[\ell_2(r(X))] + \hat{\mathbb{E}}_{\text{de}}^j[\ell_1(r(X))] - C\hat{\mathbb{E}}_{\text{nu}}^j[\ell_1(r(X))] + \lambda\mathcal{R}(r)\}$ .  
        **else**  
            Gradient ascent: set gradient  $\nabla_r \{-\hat{\mathbb{E}}_{\text{de}}^j[\ell_1(r(X))] + C\hat{\mathbb{E}}_{\text{nu}}^j[\ell_1(r(X))] + \lambda\mathcal{R}(r)\}$ .  
        **end if**  
        Update  $r$  with the gradient and the learning rate  $\gamma$ .  
    **end for**  
**end while**

---

## D Network Structure used in Sections 5 and 6

We explain the structures of neural networks used in the experiments.

### D.1 Network Structure used in Sections 5

In Section 5, we used CIFAR-10 datasets. The model was a convolutional net (Springenberg et al., 2015):  $(32 \times 32 \times 3) - C(3 \times 6, 3) - C(3 \times 16, 3) - 128 - 84 - 1$ , where the input is a  $32 \times 32$  RGB image,  $C(3 \times 6, 3)$  indicates that 3 channels of  $3 \times 6$  convolutions followed by ReLU is used. This structure has been adopted from the tutorial of Paszke et al. (2019).

### D.2 Network Structure used in Sections 6

**Inlier-based Outlier Detection:** We used the same LeNet-type CNNs proposed in Ruff et al. (2020). In the CNNs, each convolutional module consists of a convolutional layer followed by leaky ReLU activations with leakiness  $\alpha = 0.1$  and  $(2 \times 2)$ -max-pooling. For MNIST, we employ a CNN with two modules:  $(32 \times 32 \times 3) - C(3 \times 32, 5) - C(32 \times 64, 5) - C(64 \times 128, 5) - 1$ . For CIFAR-10 we employ the following architecture:  $(32 \times 32 \times 1) - C(1 \times 8, 5) - C(8 \times 4, 5) - 1$  with a batch normalization (Ioffe & Szegedy, 2015) after each convolutional layer.

The WRN architecture was proposed in Zagoruyko & Komodakis (2016) and it is also used in Golan & El-Yaniv (2018). This structure improved the performance of image recognition by decreasing the depth and increasing the width of the residual networks (Kaiming He & Sun, 2015). We omit the detailed description of the structure here.

**Covariate Shift Adaptation:** We used the 5-layer perceptron with ReLU activations. The structure is 10000-1000-1000-1000-1.

## E Existing Methods for Anomaly Detection

This section introduces the existing methods for anomaly detection. DeepSAD is a method for semi-supervised anomaly detection, which tries to take advantage of labeled anomalies (Ruff et al., 2020). GT proposed by Golan & El-Yaniv (2018) trains neural networks based on a self-labeled dataset by performing 72 geometric transformations. The anomaly score based on GT is calculated based on the Dirichlet distribution obtained by maximum likelihood estimation using the softmax output from the trained network.

In the problem setting of the DeepSAD, we have access to a small pool of labeled samples, e.g. a subset verified by some domain expert as being normal or anomalous. In the experimental results shown in Ruff et al. (2020) indicate that, when we can use such samples, the DeepSAD outperforms the other methods. However, in our experimental results, such samples are not assumed to be available, hence the method does not perform well. The problem setting of Ruff et al. (2020) and ours are both termed *semi-supervised learning* in anomaly detection, but the two settings are different.

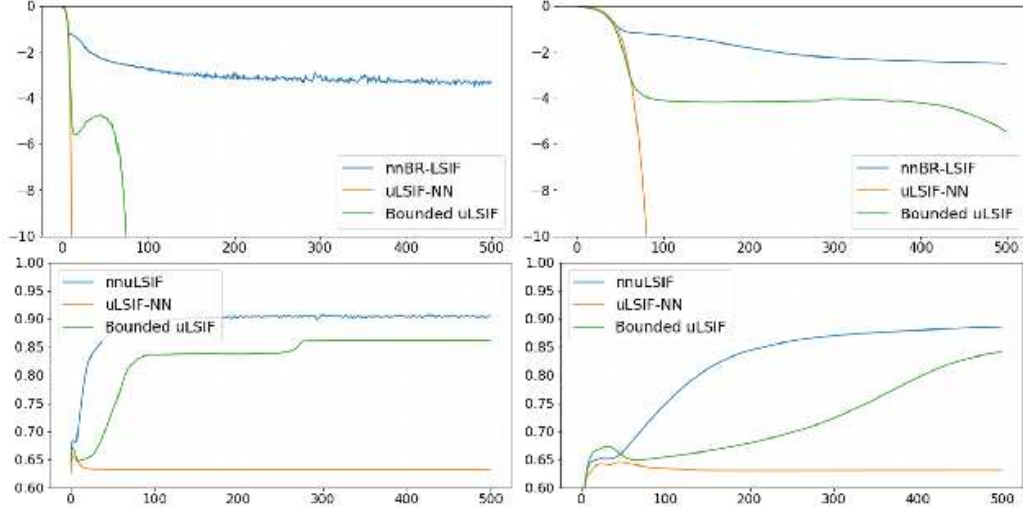


Figure 2: The learning curves of the experiments in Section 5.1. The horizontal axis is epoch. The vertical axes of the top figures indicate the training losses. The vertical axes of the bottom figures show the AURPC for the test data. The bottom figures are identical to the ones displayed in Section 5.1.

## F Details of Experiments

The details of experiments are shown in this section. The description of the data is as follows:

**MNIST:** The MNIST database is one of the most popular benchmark datasets for image classification, which consists of  $28 \times 28$  pixel handwritten digits from 0 to 9 with 60,000 train samples and 10,000 test samples (LeCun et al., 1998).

**CIFAR-10:** The CIFAR-10 dataset consists of 60,000 color images of size  $32 \times 32$  from 10 classes, each having 6000. There are 50,000 training images and 10,000 test images (Krizhevsky et al., 2012).

**fashion-MNIST:** The fashion-MNIST dataset consists of 70,000 grayscale images of size  $28 \times 28$  from 10 classes. There are 60,000 training images and 10,000 test images (Xiao et al., 2017).

**Amazon Review Dataset:** Blitzer et al. (2007) published the text data of Amazon review. The data originally consists of a rating (0-5 stars) for four different genres of products in the electronic commerce site Amazon.com: books, DVDs, electronics, and kitchen appliances. Blitzer et al. (2007) also released the pre-processed and balanced data of the original data. The pre-processed data consists of text data with four labels 1, 2, 4, and 5. We map the text data into 10,000 dimensional data by the TF-IDF mapping with that vocabulary size. In the experiment, for the pre-processed data, we solve the regression problem where the text data are the inputs and the ratings 1, 2, 4, and 5 are the outputs. When evaluating the performance, following Menon & Ong (2016), we calculate PD ( $=1-\text{AUROC}$ ) by regarding 4 and 5 ratings as positive labels and 1 and 2 ratings as negative labels.

### F.1 Experiments with Image Data

We show the additional results of Section 5. Figure 2, we show the training loss of LSIF-based methods to demonstrate the overfitting phenomenon caused by the objective function without a lower bound. In Figure 2, even though the training loss of uLSIF-NN and that of bounded uLSIF decrease more rapidly than that of nnBR-LSIF, the test AUROC score (the higher the better) either drops or fails to increase. These graphs are the manifestations of the severe overfitting in DRE without our proposed device. Figure 3 shows the experimental results of Sections 5.2 and 5.3.

### F.2 Experiments of Inlier-based Outlier Detection

In Table 4, we show the full results of inlier-based outlier detection. In almost all the cases, D3RE for inlier-based outlier detection outperforms the other methods. As explained in Section E, we consider that DeepSAD does not work well because the method assumes the availability of the labeled anomaly data, which is not available in our problem setting.



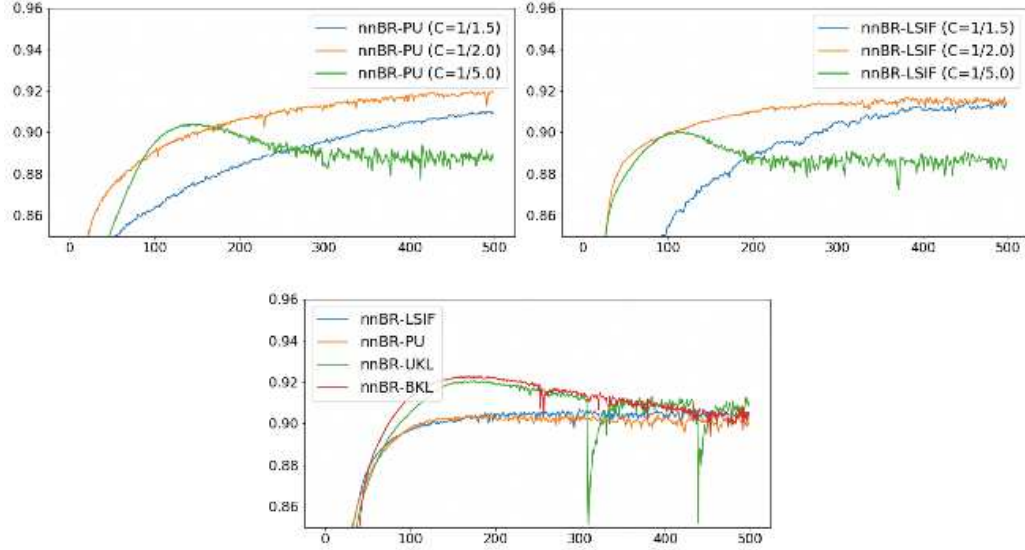


Figure 3: Top figures: the detailed experimental results for Section 5.2. Bottom figure: the detailed experimental results for Section 5.3. The horizontal axis is epoch, and the vertical axis is AUROC.

**Remark 3** (Benchmark Methods). Although GT is outperformed by our proposed method, the problem setting for the comparison is not in favor of GT as it does not assume the access to the test data. Recently proposed methods for semi-supervised anomaly detection by Ruff et al. (2020) did not perform well without using other side information used in Ruff et al. (2020). On the other hand, there is no other competitive methods in this problem setting, to the best of our knowledge.

### F.3 Experiments of Covariate Shift Adaptation

In Table 5, we show the detailed results of experiments of covariate shift adaptation. Even when the training data and the test data follow the same distribution, the covariate shift adaptation based on D3RE improves the mean PD. We consider that this is because the importance weighting emphasizes the loss in the empirical higher-density regions of the test examples.

## G Other Applications

In this section, we explain other potential applications of the proposed method.

**$f$ -divergence Estimation:**  $f$ -divergences (Ali & Silvey, 1966; Csiszár, 1967) are the discrepancy measures of probability densities based on the density ratio, hence the proposed method can be used for their estimation. They include the KL divergence (Kullback & Leibler, 1951), the Hellinger distance (Hellinger, 1909), and the Pearson divergence (Pearson, 1900), as examples.

**Two-sample Homogeneity Test:** The purpose of a homogeneity test is to determine if two or more datasets come from the same distribution (Loevinger, 1948). For two-sample testing, using a semiparametric  $f$ -divergence estimator with nonparametric density ratio models has been studied (Keziou., 2003; Keziou & Leoni-Aubin, 2005). Kanamori et al. (2010) and Sugiyama et al. (2011a) employed direct DRE for the nonparametric DRE.

**Generative Adversarial Networks:** Generative adversarial networks (GANs) are successful deep generative models, which learns to generate new data with the same distribution as the training data Goodfellow et al. (2014). Various GAN methods have been proposed, amongst which Nowozin et al. (2016) proposed  $f$ -GAN, which minimizes the variational estimate of  $f$ -divergence. Uehara et al. (2016) extended the idea of Nowozin et al. (2016) to use BR divergence minimization for DRE. The estimator proposed in this paper also has a potential to improve the method of Uehara et al. (2016).

Table 4: Average area under the ROC curve (Mean) of anomaly detection methods averaged over 5 trials with the standard deviation (SD). For all datasets, each model was trained on the single class, and tested against all other classes. The best performing method in each experiment is in bold. *SD*: Standard deviation.

MNIST Network	uLSIF-NN LeNet		nnBR-LSIF LeNet		nnBR-PU LeNet		nnBR-LSIF WRN		nnBR-PU WRN		Deep SAD LeNet		GT WRN	
Inlier Class	Mean	SD	Mean	SD	Mean	SD	Mean	SD	Mean	SD	Mean	SD	Mean	SD
0	0.999	0.000	0.997	0.000	0.999	0.000	<b>1.000</b>	0.000	<b>1.000</b>	0.000	0.592	0.051	0.963	0.002
1	<b>1.000</b>	0.000	0.999	0.000	<b>1.000</b>	0.000	<b>1.000</b>	0.000	<b>1.000</b>	0.000	0.942	0.016	0.517	0.039
2	0.997	0.001	0.994	0.000	0.997	0.001	<b>1.000</b>	0.000	<b>1.000</b>	0.001	0.447	0.027	0.992	0.001
3	0.997	0.000	0.995	0.001	0.998	0.000	<b>1.000</b>	0.000	<b>1.000</b>	0.000	0.562	0.035	0.974	0.001
4	0.998	0.000	0.997	0.001	0.999	0.000	<b>1.000</b>	0.000	<b>1.000</b>	0.000	0.646	0.015	0.989	0.001
5	0.997	0.000	0.996	0.001	0.998	0.000	<b>1.000</b>	0.000	<b>1.000</b>	0.000	0.502	0.046	0.990	0.001
6	0.997	0.001	0.997	0.001	0.999	0.000	<b>1.000</b>	0.000	<b>1.000</b>	0.000	0.671	0.027	0.998	0.000
7	0.996	0.001	0.993	0.001	0.998	0.001	<b>1.000</b>	0.000	<b>1.000</b>	0.001	0.685	0.032	0.927	0.004
8	0.997	0.000	0.994	0.001	0.997	0.000	<b>0.999</b>	0.000	<b>0.999</b>	0.000	0.654	0.026	0.949	0.002
9	0.993	0.002	0.990	0.002	0.994	0.001	<b>0.998</b>	0.001	<b>0.998</b>	0.001	0.786	0.021	0.989	0.001

CIFAR-10 Network	uLSIF-NN LeNet		nnBR-LSIF LeNet		nnBR-PU LeNet		nnBR-LSIF WRN		nnBR-PU WRN		Deep SAD LeNet		GT WRN	
Inlier Class	Mean	SD	Mean	SD	Mean	SD	Mean	SD	Mean	SD	Mean	SD	Mean	SD
plane	0.745	0.056	0.934	0.002	<b>0.943</b>	0.001	0.925	0.004	0.923	0.001	0.627	0.066	0.697	0.009
car	0.758	0.078	0.957	0.002	<b>0.968</b>	0.001	0.965	0.002	0.960	0.001	0.606	0.018	0.962	0.003
bird	0.768	0.012	0.850	0.007	<b>0.878</b>	0.004	0.844	0.004	0.858	0.004	0.404	0.006	0.752	0.002
cat	0.745	0.037	0.820	0.003	<b>0.856</b>	0.002	0.810	0.009	0.841	0.002	0.517	0.018	0.727	0.014
deer	0.758	0.036	0.886	0.004	<b>0.909</b>	0.002	0.864	0.008	0.872	0.002	0.704	0.052	0.863	0.014
dog	0.728	0.103	0.875	0.004	<b>0.906</b>	0.002	0.887	0.005	0.896	0.002	0.490	0.025	0.873	0.002
frog	0.750	0.060	0.944	0.003	<b>0.958</b>	0.001	0.948	0.004	0.948	0.001	0.744	0.014	0.879	0.008
horse	0.782	0.048	0.928	0.003	0.948	0.002	0.921	0.007	0.927	0.002	0.519	0.015	<b>0.953</b>	0.001
ship	0.780	0.048	0.958	0.003	<b>0.965</b>	0.001	0.964	0.002	0.957	0.001	0.430	0.062	0.921	0.009
truck	0.708	0.081	0.939	0.003	<b>0.955</b>	0.001	0.952	0.003	0.949	0.001	0.393	0.008	0.911	0.003

FMNIST Network	uLSIF-NN LeNet		nnBR-LSIF LeNet		nnBR-PU LeNet		nnBR-LSIF WRN		nnBR-PU WRN		Deep SAD LeNet		GT WRN	
Inlier Class	Mean	SD	Mean	SD	Mean	SD	Mean	SD	Mean	SD	Mean	SD	Mean	SD
T-shirt/top	0.960	0.005	0.981	0.001	<b>0.985</b>	0.000	0.984	0.001	0.982	0.000	0.558	0.031	0.890	0.007
Trouser	0.961	0.010	0.998	0.000	<b>1.000</b>	0.000	0.998	0.000	0.998	0.000	0.758	0.022	0.974	0.004
Pullover	0.944	0.012	0.976	0.001	0.980	0.001	<b>0.983</b>	0.002	0.972	0.001	0.617	0.046	0.902	0.005
Dress	0.973	0.006	0.986	0.001	<b>0.992</b>	0.000	0.991	0.001	0.986	0.000	0.525	0.038	0.843	0.014
Coat	0.958	0.006	0.978	0.001	<b>0.983</b>	0.000	0.981	0.002	0.974	0.000	0.627	0.029	0.885	0.003
Sandal	0.968	0.011	0.997	0.001	<b>0.999</b>	0.000	<b>0.999</b>	0.000	<b>0.999</b>	0.000	0.681	0.023	0.949	0.005
Shirt	0.919	0.005	0.952	0.001	<b>0.958</b>	0.001	0.944	0.005	0.932	0.001	0.618	0.015	0.842	0.004
Sneaker	0.991	0.001	0.994	0.002	<b>0.998</b>	0.000	<b>0.998</b>	0.000	<b>0.998</b>	0.000	0.802	0.054	0.954	0.006
Bag	0.980	0.005	0.994	0.001	<b>0.999</b>	0.000	0.998	0.000	<b>0.999</b>	0.000	0.447	0.034	0.973	0.006
Ankle boot	0.992	0.001	0.985	0.015	<b>0.999</b>	0.000	0.997	0.000	0.996	0.000	0.583	0.023	0.996	0.000

Table 5: Average PD (Mean) with standard deviation (SD) over 10 trials with different seeds per method. The best performing method in terms of the mean PD is specified by bold face.

Domains (Train → Test)	book → books		dvd → books		dvd → dvd		elec → books		elec → dvd	
DRE method	Mean	SD	Mean	SD	Mean	SD	Mean	SD	Mean	SD
w/o IW	0.093	0.003	0.128	0.008	0.100	0.005	0.212	0.012	0.187	0.008
Kernel uLSIF	0.089	0.002	0.114	0.006	0.094	0.004	0.200	0.009	0.179	0.006
Kernel KLIEP	0.089	0.002	0.116	0.006	0.094	0.004	0.205	0.011	0.184	0.008
uLSIF-NN	0.093	0.003	0.128	0.008	0.100	0.005	0.212	0.012	0.187	0.008
PU-NN	0.093	0.003	0.128	0.008	0.100	0.005	0.212	0.012	0.187	0.008
nnBR-LSIF	<b>0.086</b>	0.002	<b>0.113</b>	0.005	<b>0.091</b>	0.004	<b>0.199</b>	0.009	<b>0.176</b>	0.005
nnBR-PU	0.090	0.003	<b>0.113</b>	0.006	0.096	0.004	<b>0.199</b>	0.009	<b>0.176</b>	0.006

Domains (Train → Test)	elec → elec		kitchen → books		kitchen → dvd		kitchen → elec		kitchen → kitchen	
DRE method	Mean	SD	Mean	SD	Mean	SD	Mean	SD	Mean	SD
w/o IW	0.079	0.005	0.202	0.013	0.185	0.006	0.073	0.004	0.062	0.002
Kernel uLSIF	0.072	0.003	0.192	0.007	0.178	0.008	0.071	0.003	0.060	0.003
Kernel KLIEP	0.072	0.003	0.195	0.005	0.182	0.007	0.072	0.004	0.060	0.002
uLSIF-NN	0.079	0.005	0.202	0.013	0.185	0.006	0.073	0.004	0.062	0.002
PU-NN	0.079	0.005	0.202	0.013	0.185	0.006	0.073	0.004	0.062	0.002
nnBR-LSIF	<b>0.071</b>	0.003	<b>0.189</b>	0.008	<b>0.174</b>	0.008	<b>0.068</b>	0.003	<b>0.058</b>	0.003
nnBR-PU	0.074	0.004	0.190	0.008	<b>0.174</b>	0.008	<b>0.068</b>	0.003	0.062	0.005

**Off-policy Evaluation with External Validity:** In applications such as advertisement design selection, personalized medicine, search engines, and recommendation systems, evaluating and learning a new policy from historical data is a common problem (Beygelzimer & Langford, 2009; Li et al., 2010; Athey & Wager, 2017). To accomplish this goal, *off-policy evaluation* (OPE) evaluates a new policy by estimating the expected reward of the new policy (Dudík et al., 2011; Wang et al., 2017; Narita et al., 2019; Bibaut et al., 2019; Kallus & Uehara, 2019; Oberst & Sontag, 2019). Recently, Kato et al. (2020) proposed using covariate shift adaptation to solve the *external validity* problem in OPE, i.e., the case that the distribution of covariates is the same between the historical and evaluation data (Cole & Stuart, 2010; Pearl & Bareinboim, 2014).

**Change Point Detection:** The methods for *change-point detection* try to detect abrupt changes in time-series data (Basseville & Nikiforov, 1993; Gustafsson, 2000; Brodsky & Darkhovsky, 1993). There are two types of problem settings in change-point detection, namely the real-time detection (Adams, 2007; Garnett et al., 2009; Paquet, 2007) and the retrospective detection (Basseville & Nikiforov, 1993; Yamanishi & Takeuchi, 2002). In retrospective detection, which requires longer reaction periods, Liu et al. (2012) proposed using techniques of direct DRE. Whereas the existing methods rely on linear-in-parameter models, our proposed method enables us to employ more complex models for change point detection.

**Similarity-based Sentiment Analysis:** Kato (2019) used the density ratio estimated from PU learning for sentiment analysis of text data based on similarity.

## H Estimation error bound

The estimation error bound can be proved by building upon the proof techniques in Kiryo et al. (2017); Lu et al. (2020).

**Notations for the Theoretical Analysis:** We denote the set of real values by  $\mathbb{R}$  and that of positive integers by  $\mathbb{N}$ . Let  $\mathcal{X} \subset \mathbb{R}^d$ . Let  $p_{\text{nu}}(x)$  and  $p_{\text{de}}(x)$  be probability density functions over  $\mathcal{X}$ , and assume that the density ratio  $r^*(x) := \frac{p_{\text{nu}}(x)}{p_{\text{de}}(x)}$  is existent and bounded:  $\bar{R} := \|r^*\|_\infty < \infty$ . Assume  $0 < C < \frac{1}{\bar{R}}$ . Since  $\bar{R} \geq 1$  (because  $1 = \int p_{\text{de}}(x)r^*(x)dx \leq 1 \cdot \|r^*\|_\infty$ ), we have  $C \in (0, 1]$  and hence  $p_{\text{mod}} := p_{\text{de}} - Cp_{\text{nu}} > 0$ .

**Problem Setup:** Let the hypothesis class of density ratio be  $\mathcal{H} \subset \{r : \mathbb{R}^D \rightarrow (b_r, B_r) =: I_r\}$ , where  $0 \leq b_r < \bar{R} < B_r$ . Let  $f : I_r \rightarrow \mathbb{R}$  be a twice continuously-differentiable convex function with a bounded derivative. Define  $\tilde{f}$  by  $\partial f(t) = C(\partial f(t)t - f(t)) + \tilde{f}(t)$ , where  $\partial f$  is the derivative of  $f$  continuously extended to 0 and  $B_r$ . By denoting the loss functions  $\ell_1(t) := \partial f(t)t - f(t)$  and  $\ell_2(t) := -\tilde{f}(t)$ , we can write the risk functional  $\text{BR}_f$  and its modified estimator  $\widehat{\text{nnBR}}_f$  as

$$\begin{aligned} \text{BR}_f(r) &:= \mathbb{E}_{\text{de}} [\partial f(r(X))r(X) - f(r(X))] - \mathbb{E}_{\text{nu}} [\partial f(r(X))] \\ &= \mathbb{E}\hat{\mathbb{E}}_{\text{mod}} [\partial f(r(X))r(X) - f(r(X))] - \mathbb{E}_{\text{nu}} [\tilde{f}(r(X))] \\ &= \mathbb{E}\hat{\mathbb{E}}_{\text{mod}} \ell_1(r(X)) + \mathbb{E}_{\text{nu}} \ell_2(r(X)) \\ &= (\mathbb{E}_{\text{de}} - C\mathbb{E}_{\text{nu}}) \ell_1(r(X)) + \mathbb{E}_{\text{nu}} \ell_2(r(X)), \\ \widehat{\text{nnBR}}_f(r) &:= \rho \left( \hat{\mathbb{E}}_{\text{mod}} \ell_1(r(X)) \right) + \hat{\mathbb{E}}_{\text{nu}} \ell_2(r(X)) \\ &= \left( \rho((\hat{\mathbb{E}}_{\text{de}} - C\hat{\mathbb{E}}_{\text{nu}}) \ell_1(r(X)) + \hat{\mathbb{E}}_{\text{nu}} \ell_2(r(X)) \right), \end{aligned}$$

where we denoted  $\hat{\mathbb{E}}_{\text{mod}} = \hat{\mathbb{E}}_{\text{de}} - C\hat{\mathbb{E}}_{\text{nu}}$  and  $\rho$  is a consistent correction function with Lipschitz constant  $L_\rho$  (Definition 1).

**Remark 4.** The true density ratio  $r^*$  minimizes  $\text{BR}_f$ .

**Definition 1** (Consistent correction function Lu et al. (2020)). A function  $f : \mathbb{R} \rightarrow \mathbb{R}$  is called a consistent correction function if it is Lipschitz continuous, non-negative and  $f(x) = x$  for all  $x \geq 0$ .

**Definition 2** (Rademacher complexity). Given  $n \in \mathbb{N}$  and a distribution  $p$ , define the Rademacher complexity  $\mathcal{R}_n^p(\mathcal{H})$  of a function class  $\mathcal{H}$  as

$$\mathcal{R}_n^p(\mathcal{H}) := \mathbb{E}_p \mathbb{E}_\sigma \left[ \sup_{r \in \mathcal{H}} \left| \frac{1}{n} \sum_{i=1}^n \sigma_i r(X_i) \right| \right],$$

where  $\{\sigma_i\}_{i=1}^n$  are Rademacher variables (i.e., independent variables following the uniform distribution over  $\{-1, +1\}$ ) and  $\{X_i\}_{i=1}^n \stackrel{\text{i.i.d.}}{\sim} p$ .

The theorem in the paper is a special case of the following theorem with  $\rho(\cdot) := \max\{0, \cdot\}$  (in which case  $L_\rho = 1$ ).

**Theorem 2** (Estimation error bound). *Assume that  $B_\ell := \sup_{t \in I_r} \{\max\{|\ell_1(t)|, |\ell_2(t)|\}\} < \infty$ . Assume  $\ell_1$  is  $L_{\ell_1}$ -Lipschitz and  $\ell_2$  is  $L_{\ell_2}$ -Lipschitz. Assume that there exists an empirical risk minimizer  $\hat{r} \in \arg \min_{r \in \mathcal{H}} \widehat{\text{nnBR}}_f(r)$  and a population risk minimizer  $\bar{r} \in \arg \min_{r \in \mathcal{H}} \text{BR}_f(r)$ . Also assume  $\inf_{r \in \mathcal{H}} \mathbb{E} \mathbb{E}_{\text{mod}} \ell_1(r(X)) > 0$  and that  $(\rho - \text{Id})$  is  $(L_\rho - \text{Id})$ -Lipschitz. Then for any  $\delta \in (0, 1)$ , with probability at least  $1 - \delta$ , we have*

$$\begin{aligned} \text{BR}_f(\hat{r}) - \text{BR}_f(\bar{r}) &\leq 8L_\rho L_{\ell_1} \mathcal{R}_{n_{\text{de}}}^{p_{\text{de}}}(\mathcal{H}) + 8(L_\rho C L_{\ell_1} + L_{\ell_2}) \mathcal{R}_{n_{\text{nu}}}^{p_{\text{nu}}}(\mathcal{H}) \\ &\quad + 2\Phi_{(C, f, \rho)}(n_{\text{nu}}, n_{\text{de}}) + B_\ell \sqrt{8 \left( \frac{L_\rho^2}{n_{\text{de}}} + \frac{(1 + L_\rho C)^2}{n_{\text{nu}}} \right) \log \frac{1}{\delta}}, \end{aligned}$$

where  $\Phi_{(C, f, \rho)}(n_{\text{nu}}, n_{\text{de}})$  is defined as in Lemma 3.

*Proof.* Since  $\hat{r}$  minimizes  $\widehat{\text{nnBR}}_f$ , we have

$$\begin{aligned} \text{BR}_f(\hat{r}) - \text{BR}_f(\bar{r}) &= \text{BR}_f(\hat{r}) - \widehat{\text{nnBR}}_f(\hat{r}) + \widehat{\text{nnBR}}_f(\hat{r}) - \text{BR}_f(\bar{r}) \\ &\leq \text{BR}_f(\hat{r}) - \widehat{\text{nnBR}}_f(\hat{r}) + \widehat{\text{nnBR}}_f(\bar{r}) - \text{BR}_f(\bar{r}) \\ &\leq 2 \sup_{r \in \mathcal{H}} |\widehat{\text{nnBR}}_f(r) - \text{BR}_f(r)| \\ &\leq 2 \underbrace{\sup_{r \in \mathcal{H}} |\widehat{\text{nnBR}}_f(r) - \mathbb{E} \widehat{\text{nnBR}}_f(r)|}_{\text{Maximal deviation}} + 2 \underbrace{\sup_{r \in \mathcal{H}} |\mathbb{E} \widehat{\text{nnBR}}_f(r) - \text{BR}_f(r)|}_{\text{Bias}}. \end{aligned}$$

We apply McDiarmid's inequality McDiarmid (1989); Mohri et al. (2018) to the maximal deviation term. The absolute value of the difference caused by altering one data point in the maximal deviation term is bounded from above by  $2B_\ell \frac{L_\rho}{n_{\text{de}}}$  if the altered point is a sample from  $p_{\text{de}}$  and  $2B_\ell \frac{1+L_\rho C}{n_{\text{nu}}}$  if it is from  $p_{\text{nu}}$ . Therefore, McDiarmid's inequality implies, with probability at least  $1 - \delta$ , that we have

$$\begin{aligned} \sup_{r \in \mathcal{H}} |\widehat{\text{nnBR}}_f(r) - \mathbb{E} \widehat{\text{nnBR}}_f(r)| \\ \leq \underbrace{\mathbb{E} \left[ \sup_{r \in \mathcal{H}} |\widehat{\text{nnBR}}_f(r) - \mathbb{E} \widehat{\text{nnBR}}_f(r)| \right]}_{\text{Expected maximal deviation}} + B_\ell \sqrt{2 \left( \frac{L_\rho^2}{n_{\text{de}}} + \frac{(1 + L_\rho C)^2}{n_{\text{nu}}} \right) \log \frac{1}{\delta}}. \end{aligned}$$

Applying Lemma 2 to the expected maximal deviation term and Lemma 3 to the bias term, we obtain the assertion.  $\square$

The following lemma generalizes the symmetrization lemmas proved in Kiryo et al. (2017) and Lu et al. (2020).

**Lemma 2** (Symmetrization under Lipschitz-continuous modification). *Let  $0 \leq a < b$ ,  $J \in \mathbb{N}$ , and  $\{K_j\}_{j=1}^J \subset \mathbb{N}$ . Given i.i.d. samples  $\mathcal{D}_{(j,k)} := \{X_i\}_{i=1}^{n_{(j,k)}}$  each from a distribution  $p_{(j,k)}$  over  $\mathcal{X}$ , consider a stochastic process  $\hat{S}$  indexed by  $\mathcal{F} \subset (a, b)^{\mathcal{X}}$  of the form*

$$\hat{S}(f) = \sum_{j=1}^J \rho_j \left( \sum_{k=1}^{K_j} \hat{\mathbb{E}}_{(i,j)} [\ell_{(j,k)}(f(X))] \right),$$

where each  $\rho_j$  is a  $L_{\rho_j}$ -Lipschitz function on  $\mathbb{R}$ ,  $\ell_{(j,k)}$  is a  $L_{\ell_{(j,k)}}$ -Lipschitz function on  $(a, b)$ , and  $\hat{\mathbb{E}}_{(i,j)}$  denotes the expectation with respect to the empirical measure of  $\mathcal{D}_{(j,k)}$ . Denote  $S(f) := \mathbb{E} \hat{S}(f)$  where  $\mathbb{E}$  is the expectation with respect to the product measure of  $\{\mathcal{D}_{(j,k)}\}_{(j,k)}$ . Here, the index  $j$  denotes the grouping of terms due to  $\rho_j$ , and  $k$  denotes each sample average term. Then we have

$$\mathbb{E} \sup_{f \in \mathcal{F}} |\hat{S}(f) - S(f)| \leq 4 \sum_{j=1}^J \sum_{k=1}^{K_j} L_{\rho_j} L_{\ell_{(j,k)}} \mathcal{R}_{n_{(j,k)}, p_{(j,k)}}(\mathcal{F}).$$

*Proof.* First, we consider a continuous extension of  $\ell_{(j,k)}$  defined on  $(a, b)$  to  $[0, b)$ . Since the functions in  $\mathcal{F}$  take values only in  $(a, b)$ , this extension can be performed without affecting the values of  $\hat{S}(f)$  or  $S(f)$ . We extend the function by defining the values for  $x \in [0, a]$  as  $\ell_{(j,k)}(x) := \lim_{x' \downarrow a} \ell_{(j,k)}(x')$ , where the right-hand side is guaranteed to exist since  $\ell_{(j,k)}$  is Lipschitz continuous hence uniformly continuous. Then,  $\ell_{(j,k)}$  remains a  $L_{\rho_j}$ -Lipschitz continuous function on  $[0, b)$ . Now we perform symmetrization (Vapnik, 1998), deal with  $\rho_j$ 's, and then bound the symmetrized process by Rademacher complexity. Denoting independent copies of  $\{X_{(j,k)}\}$  by  $\{X_{j,k}^{(\text{gh})}\}_{(j,k)}$  and the corresponding expectations as well as the sample averages with  $^{(\text{gh})}$ ,

$$\begin{aligned}
 & \mathbb{E} \sup_{f \in \mathcal{F}} |\hat{S}(f) - S(f)| \\
 & \leq \sum_{j=1}^J \mathbb{E} \sup_{f \in \mathcal{F}} \left| \rho_j \left( \sum_{k=1}^{K_j} \hat{\mathbb{E}}_{(i,j)} \ell_{(j,k)}(f(X)) \right) - \mathbb{E}^{(\text{gh})} \rho_j \left( \sum_{k=1}^{K_j} \hat{\mathbb{E}}_{(j,k)}^{(\text{gh})} \ell_{(j,k)}(f(X^{(\text{gh})})) \right) \right| \\
 & \leq \sum_{j=1}^J \mathbb{E} \mathbb{E}^{(\text{gh})} \sup_{f \in \mathcal{F}} \left| \rho_j \left( \sum_{k=1}^{K_j} \hat{\mathbb{E}}_{(i,j)} \ell_{(j,k)}(f(X)) \right) - \rho_j \left( \sum_{k=1}^{K_j} \hat{\mathbb{E}}_{(j,k)}^{(\text{gh})} \ell_{(j,k)}(f(X^{(\text{gh})})) \right) \right| \\
 & \leq \sum_{j=1}^J L_{\rho_j} \sum_{k=1}^{K_j} \mathbb{E} \mathbb{E}^{(\text{gh})} \sup_{f \in \mathcal{F}} |\hat{\mathbb{E}}_{(i,j)} \ell_{(j,k)}(f(X)) - \hat{\mathbb{E}}_{(j,k)}^{(\text{gh})} \ell_{(j,k)}(f(X^{(\text{gh})}))| \\
 & = \sum_{j=1}^J L_{\rho_j} \sum_{k=1}^{K_j} \mathbb{E} \mathbb{E}^{(\text{gh})} \sup_{f \in \mathcal{F}} |\hat{\mathbb{E}}_{(i,j)} (\ell_{(j,k)}(f(X)) - \ell_{(j,k)}(0)) - \hat{\mathbb{E}}_{(j,k)}^{(\text{gh})} (\ell_{(j,k)}(f(X^{(\text{gh})})) - \ell_{(j,k)}(0))| \\
 & \leq \sum_{j=1}^J L_{\rho_j} \sum_{k=1}^{K_j} (2\mathcal{R}_{n_{(j,k)}, p_{(j,k)}}(\{\ell_{(j,k)} \circ f - \ell_{(j,k)}(0) : f \in \mathcal{F}\})) \\
 & \leq \sum_{j=1}^J L_{\rho_j} \sum_{k=1}^{K_j} 2 \cdot 2L_{\ell_{(j,k)}} \mathcal{R}_{n_{(j,k)}, p_{(j,k)}}(\mathcal{F}),
 \end{aligned}$$

where we applied Talagrand's contraction lemma for two-sided Rademacher complexity (Ledoux & Talagrand, 1991; Bartlett & Mendelson, 2001) with respect to  $(t \mapsto \ell_{(j,k)}(t) - \ell_{(j,k)}(0))$  in the last inequality.  $\square$

**Lemma 3** (Bias due to risk correction). *Assume  $\inf_{r \in \mathcal{H}} \mathbb{E} \hat{\mathbb{E}}_{\text{mod}} \ell_1(r(X)) > 0$  and that  $(\rho - \text{Id})$  is  $(L_{\rho - \text{Id}})$ -Lipschitz on  $\mathbb{R}$ . There exists  $\alpha > 0$  such that*

$$\begin{aligned}
 \sup_{r \in \mathcal{H}} |\widehat{\text{EnnBR}}_f(r) - \text{BR}_f(r)| & \leq (1 + C) B_\ell L_{\rho - \text{Id}} \exp \left( - \frac{2\alpha^2}{(B_\ell^2/n_{\text{de}}) + (C^2 B_\ell^2/n_{\text{nu}})} \right) \\
 & =: \Phi_{(C, f, \rho)}(n_{\text{nu}}, n_{\text{de}}).
 \end{aligned}$$

**Remark 5.** Note that we already have  $p_{\text{mod}} \geq 0$  and  $\ell_1 \geq 0$  and hence  $\inf_{r \in \mathcal{H}} \mathbb{E} \hat{\mathbb{E}}_{\text{mod}} \ell_1(r(X)) \geq 0$ . Therefore, the assumption of Lemma 3 is essentially referring to the strict positivity of the infimum. Here,  $\mathbb{E} \hat{\mathbb{E}}_{\text{mod}}$  and  $\mathbb{P}(\cdot)$  denote the expectation and the probability with respect to the joint distribution of the samples included in  $\hat{\mathbb{E}}_{\text{mod}}$ .

*Proof.* Fix an arbitrary  $r \in \mathcal{H}$ . We have

$$\begin{aligned}
 |\widehat{\text{EnnBR}}_f(r) - \text{BR}_f(r)| & \leq |\mathbb{E}[\widehat{\text{nnBR}}_f(r) - \widehat{\text{BR}}_f(r)]| \\
 & = |\mathbb{E}[\rho(\hat{\mathbb{E}}_{\text{mod}} \ell_1(r(X))) - \hat{\mathbb{E}}_{\text{mod}} \ell_1(r(X))]| \leq \mathbb{E} \left[ |\rho(\hat{\mathbb{E}}_{\text{mod}} \ell_1(r(X))) - \hat{\mathbb{E}}_{\text{mod}} \ell_1(r(X))| \right] \\
 & = \mathbb{E} \left[ \mathbb{1}_{\{\rho(\hat{\mathbb{E}}_{\text{mod}} \ell_1(r(X))) \neq \hat{\mathbb{E}}_{\text{mod}} \ell_1(r(X))\}} \cdot |\rho(\hat{\mathbb{E}}_{\text{mod}} \ell_1(r(X))) - \hat{\mathbb{E}}_{\text{mod}} \ell_1(r(X))| \right] \\
 & \leq \mathbb{E} \left[ \mathbb{1}_{\{\rho(\hat{\mathbb{E}}_{\text{mod}} \ell_1(r(X))) \neq \hat{\mathbb{E}}_{\text{mod}} \ell_1(r(X))\}} \right] \left( \sup_{s: |s| \leq (1+C)B_\ell} |\rho(s) - s| \right)
 \end{aligned}$$

where  $\mathbb{1}\{\cdot\}$  denotes the indicator function, and we used  $|\hat{\mathbb{E}}_{\text{mod}}\ell_1(r(X))| \leq (1+C)B_\ell$ . Further, we have

$$\begin{aligned} \sup_{s:|s|\leq(1+C)B_\ell} |\rho(s) - s| &\leq \sup_{s:|s|\leq(1+C)B_\ell} |(\rho - \text{Id})(s) - (\rho - \text{Id})(0)| + |(\rho - \text{Id})(0)| \\ &\leq \sup_{s:|s|\leq(1+C)B_\ell} L_{\rho-\text{Id}}|s - 0| + 0 \leq (1+C)B_\ell L_{\rho-\text{Id}}, \end{aligned}$$

where  $\text{Id}$  denotes the identity function. On the other hand, since  $\inf_{r \in \mathcal{H}} \mathbb{E}\hat{\mathbb{E}}_{\text{mod}}\ell_1(r(X)) > 0$  is assumed, there exists  $\alpha > 0$  such that for any  $r \in \mathcal{H}$ ,  $\mathbb{E}\hat{\mathbb{E}}_{\text{mod}}\ell_1(r(X)) > \alpha$ . Therefore, denoting the support of a function by  $\text{supp}(\cdot)$ ,

$$\begin{aligned} \mathbb{E} \left[ \mathbb{1}\{\rho(\hat{\mathbb{E}}_{\text{mod}}\ell_1(r(X))) \neq \hat{\mathbb{E}}_{\text{mod}}\ell_1(r(X))\} \right] &= \mathbb{P} \left( \hat{\mathbb{E}}_{\text{mod}}\ell_1(r(X)) \in \text{supp}(\rho - \text{Id}) \right) \\ &\leq \mathbb{P} \left( \hat{\mathbb{E}}_{\text{mod}}\ell_1(r(X)) < 0 \right) \leq \mathbb{P} \left( \hat{\mathbb{E}}_{\text{mod}}\ell_1(r(X)) < \mathbb{E}\hat{\mathbb{E}}_{\text{mod}}\ell_1(r(X)) - \alpha \right) \end{aligned}$$

holds. Now we apply McDiarmid's inequality to the right-most quantity. The absolute difference caused by altering one data point in  $\hat{\mathbb{E}}_{\text{mod}}\ell_1(r(X))$  is bounded by  $\frac{B_\ell}{n_{\text{de}}}$  if the change is in a sample from  $p_{\text{de}}$  and  $\frac{CB_\ell}{n_{\text{nu}}}$  otherwise. Therefore, McDiarmid's inequality implies

$$\mathbb{P} \left( \hat{\mathbb{E}}_{\text{mod}}\ell_1(r(X)) < \mathbb{E}\hat{\mathbb{E}}_{\text{mod}}\ell_1(r(X)) - \alpha \right) \leq \exp \left( -\frac{2\alpha^2}{(B_\ell^2/n_{\text{de}}) + (C^2B_\ell^2/n_{\text{nu}})} \right).$$

□

## I Rademacher Complexity Bound

The following lemma provides an upper-bound on the Rademacher complexity for multi-layer perceptron models in terms of the Frobenius norms of the parameter matrices. Alternatively, other approaches to bound the Rademacher complexity can be employed. The assertion of the lemma follows immediately from the proof of Theorem 1 of Golowich et al. (2019) after a slight modification to incorporate the absolute value function in the definition of Rademacher complexity.

**Lemma 4** (Rademacher complexity bound (Golowich et al., 2019, Theorem 1)). *Assume the distribution  $p$  has a bounded support:  $B_p := \sup_{x \in \text{supp}(p)} \|x\| < \infty$ . Let  $\mathcal{H}$  be the class of real-valued networks of depth  $L$  over the domain  $\mathcal{X}$ , where each parameter matrix  $W_j$  has Frobenius norm at most  $B_{W_j} \geq 0$ , and with 1-Lipschitz activation functions  $\varphi_j$  which are positive-homogeneous (i.e.,  $\varphi_j$  is applied element-wise and  $\varphi_j(\alpha t) = \alpha \varphi_j(t)$  for all  $\alpha \geq 0$ ). Then*

$$\mathcal{R}_n^p(\mathcal{H}) \leq \frac{B_p \left( \sqrt{2 \log(2)L} + 1 \right) \prod_{j=1}^L B_{W_j}}{\sqrt{n}}.$$

*Proof.* The assertion immediately follows once we modify the beginning of the proof of Theorem 1 by introducing the absolute value function inside the supremum of the Rademacher complexity as

$$\mathbb{E}_\sigma \left[ \sup_{r \in \mathcal{H}} \left| \sum_{i=1}^n \sigma_i r(x_i) \right| \right] \leq \frac{1}{\lambda} \log \mathbb{E}_\sigma \sup_{r \in \mathcal{H}} \exp \left( \lambda \left| \sum_{i=1}^n \sigma_i r(x_i) \right| \right).$$

for  $\lambda > 0$ . The rest of the proof is identical to that of Theorem 1 of Golowich et al. (2019). □

## J Strong convexity and $L^2$ error bound

An estimation error bound in terms of  $\text{BR}_f$  can be converted to that of an  $L^2$  distance when the true density ratio and the density ratio model are square-integrable and  $f$  is strongly convex.

**Lemma 5** ( $L^2$  distance bound). *Let  $\mathcal{H} := \{r : \mathcal{X} \rightarrow (b_r, B_r) =: I_r \mid \int |r(x)|^2 d\mathbf{x} < \infty\}$  and assume  $r^* \in \mathcal{H}$ . If  $\inf_{t \in I_r} f''(t) > 0$ , then there exists  $\mu > 0$  such that for all  $r \in \mathcal{H}$ ,*

$$\|r - r^*\|_{L^2(p_{\text{de}})}^2 \leq \frac{2}{\mu} (\text{BR}_f(r) - \text{BR}_f(r^*))$$

*holds.*

*Proof.* Since  $\mu := \inf_{t \in I_r} f''(t) > 0$ , the function  $f$  is  $\mu$ -strongly convex. By the definition of strong convexity,

$$\begin{aligned} \text{BR}_f(r) - \text{BR}_f(r^*) &= (\text{BR}_f(r) - \mathbb{E}_{\text{de}} f(r^*(X))) - \underbrace{(\text{BR}_f(r^*) + \mathbb{E}_{\text{de}} f(r^*(X)))}_{=0} \\ &= \mathbb{E}_{\text{de}} [f(r^*(X)) - f(r(X)) + \partial f(r(X))(r^*(X) - r(X))] \\ &\geq \mathbb{E}_{\text{de}} \left[ \frac{\mu}{2} (r^*(X) - r(X))^2 \right] = \frac{\mu}{2} \|r^* - r\|_{L^2(p_{\text{de}})}^2. \end{aligned}$$

□

**Lemma 6** ( $\ell_2$  distance bound). *Fix  $r \in \mathcal{H}$ . Given  $n$  samples  $\{x_i\}_{i=1}^n$  from  $p_{\text{de}}$ , with probability at least  $1 - \delta$ , we have*

$$\frac{1}{n} \sum_{i=1}^n (r(x_i) - r^*(x_i))^2 \leq \underbrace{\mathbb{E} [(r - r^*)^2(X)]}_{= \|r - r^*\|_{L^2(p_{\text{de}})}^2} + (2\bar{R})^2 \sqrt{\frac{\log \frac{1}{\delta}}{2n}}.$$

*Proof.* The assertion follows from McDiarmid's inequality after noting that altering one sample results in an absolute change bounded by  $\frac{1}{n}(2\bar{R})^2$ . □